International
Progress Report

IPR-01-52

Äspö Hard Rock Laboratory

TRUE Block Scale
Detailed characterisation stage

Interference tests and tracer tests
PT-1 PT-4

Peter Andersson
Jan-Erik Ludvigson
Eva Wass
Magnus Holmqvist

GEOSIGMA AB

September 1999

Svensk Kärnbränslehantering AB
Swedish Nuclear Fuel
and Waste Management Co
Box 5864
SE-102 40 Stockholm Sweden
Tel +46 8 459 84 00
Fax +46 8 661 57 19

Äspö Hard Rock
Laboratory

Report no.
IPR-01-52

No.
F56K

Author
Andersson, Ludvigson,
Wass, Holmqvist

Date
99-09-01

Checked by

Date

Approved
Christer Svemar

Date
02-08-23

Äspö Hard Rock Laboratory

TRUE Block Scale
Detailed characterisation stage

Interference tests and tracer tests
PT-1 PT-4

Peter Andersson
Jan-Erik Ludvigson
Eva Wass
Magnus Holmqvist

GEOSIGMA AB

September 1999

Keywords: TRUE, block scale, tracer tests, tracer dilution test, interference test

Abstract

One of the components of the TRUE Block Scale Detailed Characterisation Stage (DCS) is to conduct a combined interference and tracer test programme (pre-tests) in the instrumented Block Scale array within the Äspö HRL. The overall objectives of the pre-tests (PT-1 to PT-4) were to test the present deterministic structural model, March 99 model and to test the possibility to conduct tracer tests with injection of tracer in points belonging to the network of deterministic (discrete) structures. In total four interference tests were performed with a duration of 1-28 days. Flow measurements using the tracer dilution technique was performed simultaneously in 6-12 observation sections during the long-term interference tests. Tracer injections were made in four observation sections during the last test (PT-4). The flow and pressure responses obtained during the tests confirmed the deterministic structural model. Tracer breakthrough was obtained from all four injection points. The tracer test results were used to estimate transport parameters for three flow paths involving one to three structures within the block.

Sammanfattning

En av komponenterna av TRUE Block Scale Detailed Characterisation Stage (DCS) är att utföra ett kombinerat interferens- och spårämnestestprogram (för-tester) i den instrumenterade Block Scale-området av Äspö HRL. Det övergripande syftet med för-testerna (PT-1 till PT-4) är att testa den aktuella strukturmodellen, Mars ’99-modellen, och att då testa möjligheten att utföra spårämnesförsök med injicering av spårämnen i punkter tillhörande nätverket av deterministiska (diskreta) strukturer. Totalt utfördes fyra interferenstester med en varaktighet av 1-28 dagar. Under de längre försöken utfördes samtidiga flödesmätningar med spårämnesteknik i 6-12 observationssektioner. I det sista testet, PT-4, injicerades spårämnen i fyra observationssektioner. Beräknade flödes- och tryckresponser, erhållna under försöken, bekräftade den aktuella strukturmodellen. Genombrott av spårämne uppnåddes från alla fyra injektionspunkterna. Resultaten användes för att bestämma transportparametrar för tre flödesvägar involverande en till tre strukturer i blocket.

Executive Summary

The Second phase of the Detailed Characterisation Stage (DCS II) of the TRUE Block Scale Project is currently ongoing at Äspö HRL. The primary purpose of DCS II is to explore the possibilities to perform tracer tests in the selected target volume at Äspö HRL. This is accomplished by updating the flow model though different field activities and by performing scoping calculations (Winberg, in prep.).

The purpose of the pre-tests was to assess the possibility to perform quantitative and informative tracer experiments in the current borehole array. The tests also served as a check of the current structural model, March 99 model (Hermanson in prep.) and as input to whether an additional borehole was needed or not. The four pre-tests (PT-1 to PT-4) included a combination of flow and pressure interference tests similar to the ones performed in the Preliminary Characterisation Stage (PCS) (Andersson et al., 1998). The main difference was the existence of the new borehole KI0025F02 and maximum strength in sinks.

The pre-tests in selected sections involved four different test set-ups, three runs with tracer dilution tests combined with pumping (PT-1 to PT-3) and a tracer test (PT-4). The test cycle for PT-1 to PT-3 was similar to the one used in the combined interference and tracer tests performed in the Preliminary Characterisation Stage (PCS) (Andersson et al., 1998).

The pumping and recovery phases were performed as conventional constant head interference tests implying that the flow rates and pressures were monitored with a high measurement frequency. The flow from the pumped section together with the electrical conductivity was measured manually during the pumping period.

The pre-test #4, PT-4, was focused on tracer transport and performed as a radially converging tracer test. Based on the many good flow responses during PT-2 the same set-up was decided for use in PT-4. Tracer injections were made in four sections (KA2563A:S1, KA2563A:S4, KI0025F02:P3 and KI0025F02:P6) with pumping in section KI0023B:P6 using the same pumping rate as in PT-2. The tracer injections were performed as decaying pulses and sampling was performed in the water withdrawn from the source section KI0023B:P6. In two of the injections, the tracer solution was exchanged with non-traced water in order to shorten the tail of the breakthrough curve. The tracers used were three different fluorescent dyes namely, Uranine (KA2563A:S1), Rhodamine WT (KA2563A:S4 and KI0025F02:P6) and Amino G Acid (KI0025F02:P3).

The three pre-tests PT-1, PT-2 and PT-3 generally confirm the March´99 structural model. In most cases, the flow and pressure responses give the same indication of connectivity, i.e. a good (high and fast) pressure response and a good flow response (increase). However, there are exceptions in each test where a low and slow pressure response is obtained together with a good flow response, or the opposite. These results imply that pressure responses alone cannot be used for assessment of transport connectivity.

PT-1, performed by pumping structure #13 (KI0023B:P4), shows good flow and pressure responses both within the structure as well as in structures #20 and #21. The only exception being section KI0025F02:P3 where a very good flow response and a slow pressure response are obtained. One possible explanation for this may be that the section is located close to a constant head boundary, which also is indicated by the quantitative interpretation of the pressure response.

PT-2 (and PT-4), performed by pumping structure #21 (KI0023B:P6), gives good flow and pressure responses in structures #6, 13, 20, 21 and #22. The only unexpected response is the significant flow response in structure #19 (KA2563A:S1) which has a relatively low and slow pressure response. Thus, connectivity between structures #21 and #19 clearly exists. This was also confirmed by the tracer breakthrough obtained during PT-4. Two sections with structures not identified in the March´99 model, KI0023B:P5 and KI0025F02:P7, also have good flow and pressure responses.

The third test, PT-3, performed by pumping structure #20 (KI0025F02:P5), has an almost identical pressure response pattern as in PT-2. Both pressure and flow responses are stronger due to the stronger sink but the pattern is identical. This indicates that KI0025F02 may be used as sink in future tracer tests and that structures #20 and #21 have a very good hydraulic connection.

The quantitative analysis of the most prominent pressure responses generally shows predominantly radial flow with a slight leakage at the end of the test. Analysis of responses in the bounding structures #6, 7 and 19 shows effects of constant head boundaries. In PT-3, indications of no flow boundaries are evident in the responses in KI0025F:R4 and KI0025F02:P7. This may indicate that structure #20 ends to the east of borehole KI0025F and the unknown structure in KI0025F02:P7 also is terminated to the west of KI0025F02.

The transmissivity and diffussivity values determined are generally rather uniform for structure #20 ($T=7\text{-}12\cdot10^{-7}$ m^2/s, $T/S=3\text{-}10$ m^2/s). They are also consistent with earlier interpretations (Andersson et al., 1998 and Adams et al., in prep.). Structure #21, only interpreted in KI0023B:P6 and KI0025F02:P3 gives a similar point value in KI0023B:P6 whereas the low and slow response in KI0025F02:P3 gives an indication of a higher transmissivity ($T=6\text{-}10\cdot10^{-6}$ m^2/s) in that region. The responses in the bounding structures #6, 7 and 19 generally yield about one order of magnitude higher transmissivity values than structures #13, 20, 21 and 22.

The tracer dilution tests in 14 different sections showed that the “natural” flow varies considerably within the block scale volume. An extremely high flow rate (10 l/h) was measured in KI0023B:P7 which constitutes a short-circuit between structures #6 and #20. The flow rates in the other measured sections were typically in the range 1-200 ml/h. Estimated hydraulic gradients using transmissivities of the sections are typically in the order of 0.3-3 m/m. The exceptions are a few sections connected to structures #20 and #21 having a lower gradient and an extremely high gradient in the short-circuit section KI0023B:P7.

The tracer test performed by pumping in structure #21 (KI0023B:P6) resulted in tracer breakthrough from all four injection points, KA2563A:R1 (structure #19), KA2563A:S4 (structure #20), KI0025F02:P3 (structures #13 and 21) and KI0025F02:P6 (structure #22).

Very high mass recovery was obtained for the injections in KI0025F03:P3 and P6 whereas the short flow path from KA2563A:S4 only gave 50% mass recovery which should be compared to 44% in a previous test (Andersson et al., 1998). The mass loss is attributed to the boundary conditions (intersections with other structures having lower hydraulic head).

The numerical modelling using a simple one-dimensional advection-dispersion model was not able to fit the breakthrough curves very well. In addition, evaluated dispersivity values where unrealistically high for a single path for two of the flow paths. Usage of a multiple-path model would improve the fits considerably although this could not be done within the framework of this evaluation. The transport parameters calculated based on the mean travel times; fracture conductivity, equivalent fracture aperture and flow porosity, show somewhat different values, where the flow path from KI0025F02:P6 shows a slow transport, indicating high flow porosity (and large equivalent aperture) whereas the fast flow path from KA2563A:S4 has about one order of magnitude lower flow porosity (and equivalent aperture).

Contents

1 Introduction

1.1 Background

The Second phase of the Detailed Characterisation Stage (DCS II) of the TRUE Block Scale Project is currently ongoing at Äspö HRL. The primary purpose of DCS II is to explore the possibilities to perform tracer tests in the selected target volume at Äspö HRL. This is accomplished by updating the flow model though different field activities and by performing scoping calculations (Winberg, in prep.). In addition, an elaborate effect is put on identifying issues for future tracer tests posing of hypotheses, and design calculations.

Recent field work has included a detailed flow logging, using the POSIVA tool, in boreholes KA2563A and KA2511A and a series of short-term flow and pressure interference tests in different sections of KA2563A in order to update the structural model and to optimise the packer configuration in the boreholes. Boreholes KA2511A and KA2563A have been re-instrumented based on these tests with a focus on the selected target structures #13 and #20.

1.2 Objectives

The purpose of the pre-tests was to assess the possibility to perform quantitative and informative tracer experiments in the current borehole array, cf. Table 1-1. The tests also served as a check of the current structural model, March 99 model (Hermanson in prep.) and as input to whether an additional borehole was needed or not. The pre-tests included a combination of flow and pressure interference tests similar to the ones performed in the Preliminary Characterisation Stage (PCS) (Andersson et al., 1998). The main difference was the existence of the new borehole KI0025F02 and maximum strength in sinks.

Table 1-1. Objectives and performance of pre-tests #1 to #5 (PT-1 to PT-5). The structural interpretation refers to the March 1999 model (Hermanson, in prep.).

Test #	Objective	Performance
PT-1	Test of connectivity within structure #13 and between #13 and #20	Tracer dilution test under natural and pumped conditions. Sink in #13 (KI0023B:P4)
PT-2	Test of connectivity within structure #20 and between #20 and #21, #22, #13, #6 and some minor structures	Tracer dilution test under natural and pumped conditions. Sink in #21 (KI0023B:P6)
PT-3	Test of connectivity within structure #20 and between #20 and #21, #22, #13, #6 and some minor structures	Tracer dilution test under natural and pumped conditions. Sink in #20 (KI0025F02:P5)
PT-4	Test of transport connectivity, assessment of transport properties	Tracer test in radially converging flow geometry. Tracer injection in 3-5 selected sections. Selection of sink and injection sections based on PT-1 to PT-3.
PT-5*	Test of connectivity within structure #19 and between #19 and #13	Tracer dilution test under natural and pumped conditions. Sink in #19 (KI0025F:R2)

*= PT-5 was postponed due to a strained time schedule.

2 Performance and evaluation procedure

2.1 Equipment and tracers used

Each of the five characterisation boreholes involved in the tests is instrumented with 6-10 inflatable packers such that 5-10 borehole sections are isolated. Each borehole section is connected to a pressure transducer which is connected the HMS-system. Each of the sections planned to be used for tracer tests are equipped with three nylon hoses, two with an inner diameter of 4 mm and one with an inner diameter of 2 mm. The two 4-mm hoses are used for injection, sampling and circulation in the borehole section whereas the 2-mm hose is used for pressure monitoring.

The tracer dilution tests were performed using six identical equipment set-ups for tracer tests, i.e. allowing six sections to be measured simultaneously. A schematic drawing of the tracer test equipment is shown in Figure 2-1. The basic idea is to have an internal circulation in the borehole section. The circulation makes it possible to obtain a homogeneous tracer concentration in the borehole section and to sample the tracer concentration outside the borehole in order to monitor the injection rate of the tracer with time, and also the dilution rate.

Circulation is controlled by a pump with variable speed (A) and measured by a flow meter (B). Water and tracer injections are made with two different HPLC plunger pumps (C1 and C2) and sampling is made by continuously extracting a small volume of water from the system through a flow controller (constant leak) to a fractional sampler (D). Water and tracer solution is stored in two separate pressurised vessels (E1 and E2) under nitrogen atmosphere. The tracer test equipment has earlier been used in the TRUE-1 tracer tests (e.g. Andersson, 1996).

The tracers used were Uranine (Sodium Fluorescein) from KEBO (purum quality), Amino G Acid from Aldrich (techn.quality) and Rhodamine WT from Holiday Dyes Inc. (techn. quality). These tracers have all been used extensively in the TRUE-1 tracer tests.

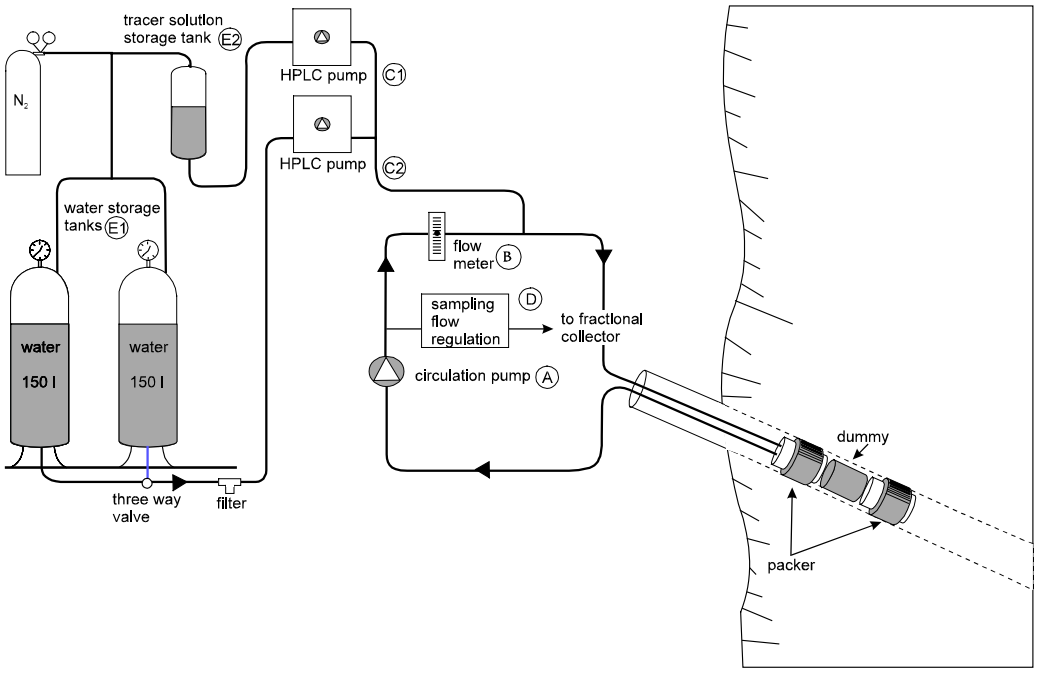

Figure 2-1. *Schematic drawing of the tracer injection/sampling system used in the TRUE Project.*

2.2 Performance of the combined interference tests and tracer tests, pre-tests #1-4 (PT-1, PT-2, PT-3, PT-4)

The pre-tests in selected sections involved four different test set-ups, three runs with tracer dilution tests combined with pumping (PT-1 to PT-3) and a tracer test (PT-4), cf. Table 1-1.

The test cycle for PT-1 to PT-3 was similar to the one used in the combined interference and tracer tests performed in the Preliminary Characterisation Stage (PCS) (Andersson et al., 1998). The following test cycle was used:

Day 1 start tracer dilution test under natural gradient in six selected sections

Day 2 change of test sections to six new locations (only PT-2 and PT-3)

Day 3 start pumping in selected sink section

Day 4 change of test section to the six first tested (only PT-2 and PT-3)

Day 5 stop pumping, preparations for the next test

PT-1 only included six sections which means that these tests had a duration of three days each and hence, a duration of the pumping period of 24 hours, cf. Table 2-1. The tracer test, PT-4, did not include any measurement during unpumped conditions. Instead the actual injection of tracers was preceded by a period of 3-5 days with pumping in the selected sink section to establish stationary flow and pressure conditions.

All sinks were established using maximum possible flow. The flow was only restricted by the dimension of the tubing and the hydraulic transmissivity of the section.

The pumping and recovery phases were performed as conventional constant head interference tests implying that the flow rates and pressures were monitored with a high measurement frequency. The logging frequency of the HMS system was manually set before start of pumping phase and recovery phase by the HMS operator. The logging frequency was set to enable transient evaluation of pressure data. This means a logging frequency of one scan every second during the first ten minutes, one scan every minute up to two hours and one scan every ten minutes up to two days.

The flow from the pumped section together with the electrical conductivity of the pumped water were measured manually during the pumping period.

The pre-test #4, PT-4, was focused on tracer transport and performed as a radially converging tracer test. Based on the many good flow responses observed during PT-2, the same set-up was decided for use in PT-4. Tracer injections were made in four sections (KA2563A:S1, KA2563A:S4, KI0025F02:P3 and KI0025F02:P6) with pumping in section KI0023B:P6 with the same pumping rate as in PT-2. The tracer injections were performed as decaying pulses and sampling was performed in the water withdrawn from the source section KI0023B:P6. In two of the injections, the tracer solution was exchanged with non-traced water in order to obtain a well-defined squared injection signal, and thus shorten the tail of the breakthrough curve.

Table 2-1 summarises the test set-ups including expected flow rates (based on earlier tests) and distances. The positions of the sinks and sections used for flow measurements using the tracer dilution technique are shown in Figures 2-2 to 2-5.

Table 2-1. Test set-ups for TRUE Block Scale pre-tests PT-1 to PT-4. The structural interpretation refers to the March 1999 model (Hermanson, in prep.).

Test #	Sink	Structure #	Test sections	Structure #	Natural flow* (ml/h)	Euclidean distance (m)
PT-1	KI0023B:P4	13	KA2563A:S3	13	?	21
			KI0025F02:P3	13	14	27
			KI0025F02:P5	20	5	22
			KA2563A:S4	20	500	26
			KI0025F:R4	20	2	41
			KI0023B:P6	21	2	15
PT-2	KI0023B:P6	21	KI0025F02:P5	20	5	20
			KA2563A:S4	20	500	16
			KI0025F:R4	20	2	42
			KI0023B:P4	13	1	15
			KI0025F02:P3	13, 21	14	36
			KA2563A:S3	13	?	21
			KI0025F02:P8	6	30	23
			KI0025F02:P6	22	?	18
			KI0023B:P7	6, 20	?	14
			KI0025F02:P7	?	?	20
			KI0023B:P5	?	?	7
			KA2563A:S1	19	?	40
PT-3	KI0025F02:P5	20	KI0023B:P6	21	2	20
			KA2563A:S4	20	500	35
			KI0025F:R4	20	2	24
			KI0023B:P4	13	1	22
			KI0025F02:P3	13, 21	14	24
			KA2563A:S3	13	?	38
			KI0025F02:P8	6	30	21
			KI0025F02:P6	22	?	7
			KI0023B:P7	6, 20	?	26
			KI0023B:P5	?	?	20
			KI0025F02:P7	?	?	15
			KI0023B:P2	19	?	43
PT-4	KI0023B:P6	21	KA2563A:S1	19	?	40
			KA2563A:S4	20	500	16
			KI0025F02:P3	13, 21	14	36
			KI0025F02:P6	22	?	18

* estimated based on earlier measurements

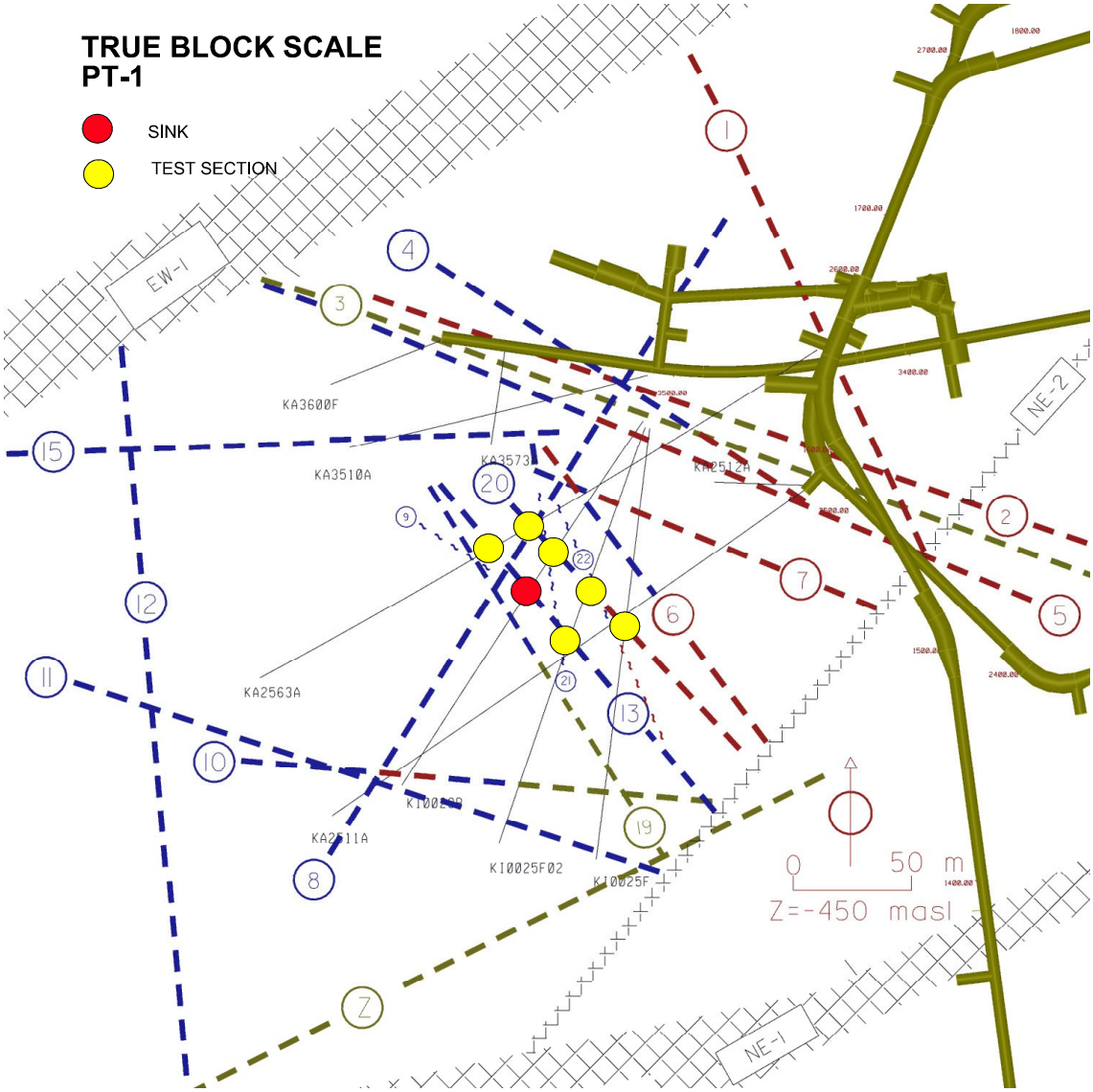

Figure 2-2. *Position of sink and dilution test sections during the TRUE Block Scale pre-test PT-1. The positions of the structures are based on the March 1999 structural model (Hermanson, in prep.). Z=-450 masl.*

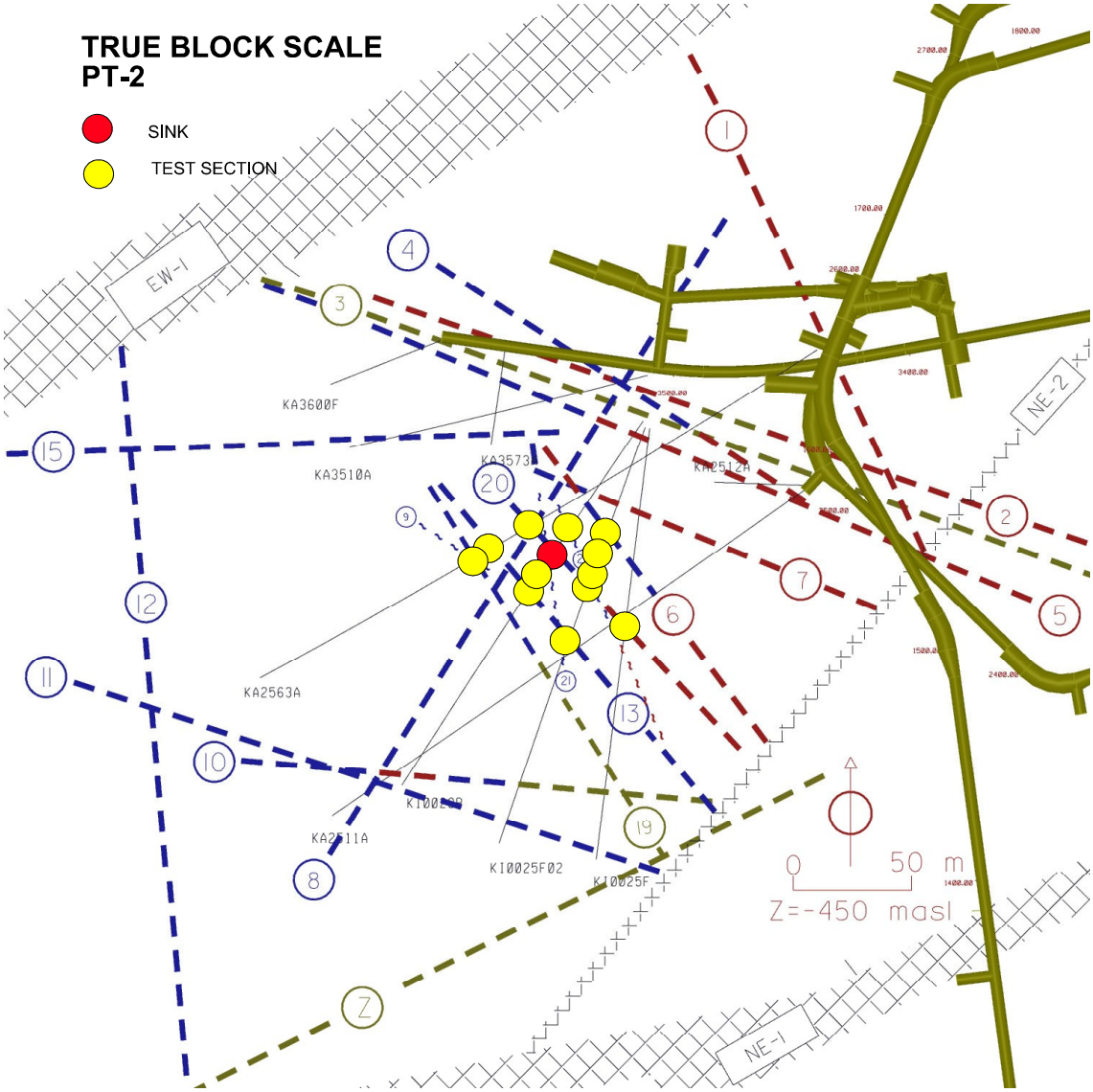

Figure 2-3. *Position of sink and dilution test sections during the TRUE Block Scale pre-test PT-2. The positions of the structures are based on the March 1999 structural model (Hermanson, in prep.). Z=-450 masl.*

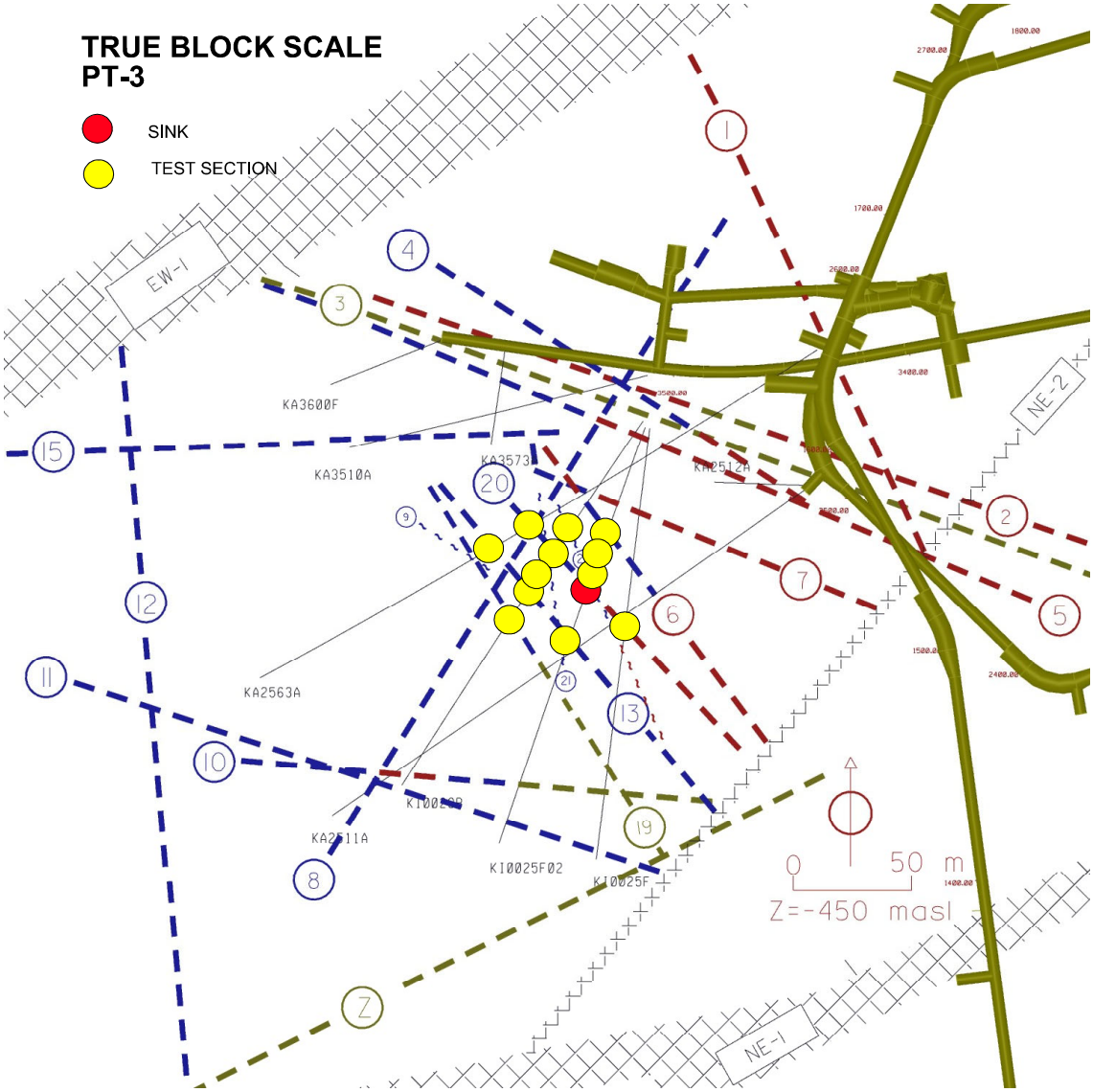

Figure 2-4. *Position of sink and dilution test sections during the TRUE Block Scale pre-test PT-3. The positions of the structures are based on the March 1999 structural model (Hermanson, in prep.). Z=-450 masl.*

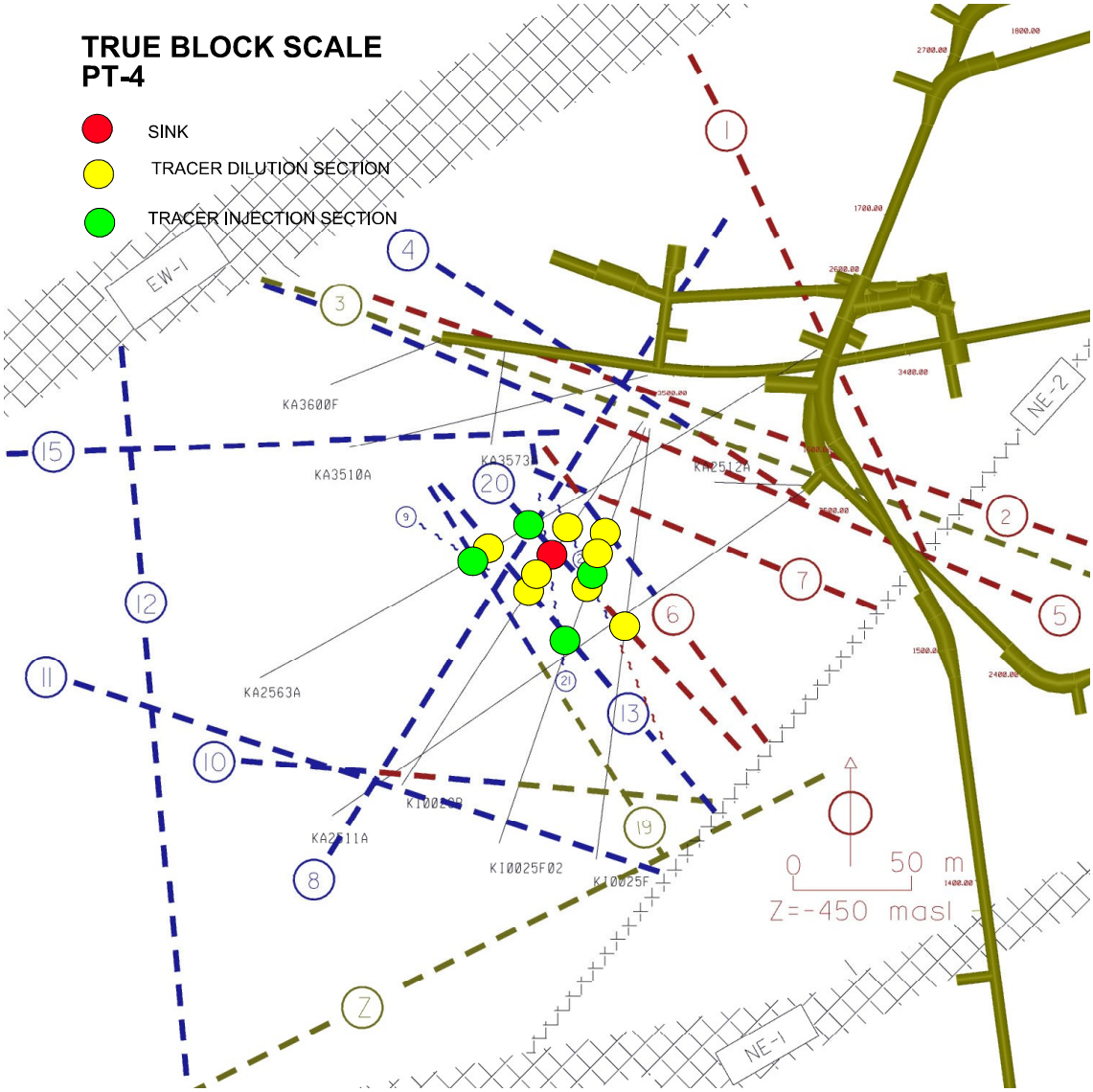

Figure 2-5. *Positions of sink, dilution test sections and tracer injection sections during the TRUE Block Scale pre-test PT-4. The positions of the structures are based on the March 1999 structural model (Hermanson, in prep.). Z=-450 masl.*

2.3 Laboratory analyses

Samples were analysed for dye tracer content at the GEOSIGMA Laboratory, Uppsala, using a Jasco FP777 Spectrofluorometer.

2.4 Evaluation

2.4.1 Hydraulic interference tests

Qualitative interpretation

The hydraulic responses have been evaluated in different steps, each at which part of the data has been sorted out for further (quantitative) evaluation. This procedure was necessary in order to restrict the quantitative evaluation to a manageable amount of data.

First, time-drawdown- and time-recovery plots were prepared for sections showing a drawdown (or recovery) of more than s_p=0.1 m (1 kPa) at the end of the tests. This threshold value was selected with due consideration of the amplitude of the tidal effects. These types of plots were used to estimate the response times (t_R) for each section. The response time is here defined as the time, after start of flowing, when a drawdown (or recovery) of 1 kPa (0.1 m) is observed (in the logarithmic plots) for the actual observation section.

To account for the different flow rates used in the tests and to make the response plots comparable between tests, the final drawdown by stop of flowing (s_p) is normalised with respect to the flow rate (Q). The ratio s_p/Q is plotted on the Y-axis. On the X-axis, the ratio of the response time to the squared distance R in space between the (midpoint of the) source section and (the midpoint of) each observation section (t_R/R^2) is plotted. The latter ratio is inversely related to the hydraulic diffusivity of the rock, which parameter indicates the speed of propagation of the pressure signal in the rock created by the drawdown in the flowing section. The distances in space between source and observation points, R, are given in Appendix 1 for all tests.

From the response plots of s_p/Q versus t_R/R^2 for each test, sections with anomalously fast response times (high hydraulic diffusivity) and large (normalised) drawdown can be identified. Such sections, showing primary responses, can be assumed to have a distinct hydraulic connection to the flowing section and may be intersected by fracture zones or other conductive structures in the rock. On the other hand, sections with delayed and weak responses may correspond to sections in the rock mass between such structures.

From the calculated values of s_p/Q (index 1) and t_R/R^2 (index 2) for each observation section, and from each test, a common response matrix, showing the response patterns for all tests, was prepared by classifying the responses by means of the above indexes 1 and -2. For index 1 the following class limits and associated characteristics of drawdown were used:

Index 1 (s_p/Q)

$s_p/Q > 1 \cdot 10^5$ s/m^2	Excellent
$3 \cdot 10^4 < s_p/Q \leq 1 \cdot 10^5$ s /m^2	High
$1 \cdot 10^4 < s_p/Q \leq 3 \cdot 10^4$ s /m^2	Medium
$s_p/Q \leq 1 \cdot 10^4$ s /m^2	Low

For index 2 the following class limits and response characteristics were used:

Index 2 (t_R/R^2)

$t_R/R^2 < 0.01$ s/m^2	Excellent (E)
$0.01 \leq t_R/R^2 < 0.1$ s/m^2	Good (G)
$0.1 \leq t_R/R^2 < 0.3$ s/m^2	Medium (M)
$t_R/R^2 \geq 0.3$ s/m^2	Bad (B)

The results from the qualitative analysis were compared with the structural (March 99) model and checked for consistency and possible need of revision. It should be pointed out that the response diagrams of s_p/Q versus t_R/R^2 described above were only meant to be used as diagnostic tools to identify the most significant responses during each test and to construct the response matrix. The diagrams should be used with some care since the true distances (along pathways) between the source and observation sections are uncertain which may affect the position of a certain section in the horizontal direction in the diagrams. However, in most cases, the shortest distance between the source and observation section, as used here, is considered as a sufficient and robust approximation for the above purpose.

Another potential source of error in the response diagrams may occur if (internal) hydraulic interaction exists between sections along an observation borehole. For example, such interaction could either be due to packer leakage (insufficient packer sealing) or leakage through interconnecting fractures around the packers. Such a condition may give a false impression that good hydraulic communication exists between such observation sections and the actual source section. However, any analysis method will suffer from this potential source of error.

The derivative of the drawdown was used as a diagnostic tool in the interpretation of the flow geometry and deduction of hydraulic boundaries. The derivative was generated by the SKB-code PUMPKONV and plotted together with the drawdown curves.

Quantitative interpretation

The main purpose of the quantitative interpretation of the interference tests in this study is to estimate the hydraulic parameters and the hydraulic characteristics of the most

significant responses during each test as identified from the qualitative interpretation. The transmissivity, storativity and hydraulic diffusivity, and in some cases also the leakage coefficient, are estimated from the tests. The estimated hydraulic parameters are assumed to represent the hydraulic properties of some of the fracture zones tested. In addition, the quantitative interpretation also provides (soft) information on the flow geometry during the tests including effects of outer hydraulic boundaries.

The quantitative interpretation (time-drawdown) was made using the code AquiferTest (Waterloo Hydrologic). As a standard interpretation model, the Hantush model for constant flow rate tests in a leaky (or non-leaky) aquifer with no aquitard storage was used. This model was used because of its generality and its ability to analyse pure radial flow (Theis' type curve) as well as leaky (pseudo-spherical) flow. The type curve for r/L=0 in the Hantush' model (no leakage) corresponds to the classical Theis' type curve for radial flow. Tests showing periods with (pseudo)-radial flow were analysed using the Cooper-Jacob's method in semi-logarithmic graphs. By the analysis of the constant head tests, a varying (declining) flow rate was applied at the sink.

2.4.2 Tracer dilution tests

Flow rates were calculated from the decay of tracer concentration versus time through dilution with natural unlabelled groundwater, c.f. Winberg (*ed*), (1996).

The dilution of tracer with time in the injection sections was determined by analysing the samples withdrawn from the sections. The so-called "dilution curves" were plotted as the natural logarithm of concentration versus time. Theoretically, a straight-line relationship exists between the natural logarithm of the relative tracer concentration (c/c_0) and time (t):

$$Q_{bh} = -V \cdot \Delta \ln (c/c_0) / \Delta t \qquad 2\text{-}1$$

where Q_{bh} (m^3/s) is the groundwater flow rate through the borehole section and V (m^3) is the volume of the borehole section. The flow, Q_{bh}, may be translated into a Darcy velocity by taking into account the distortion of the flow caused by the borehole and the angle between borehole and flow direction, c.f. Rhén et al. (1991). The relation between the flow in the rock, the Darcy velocity, q_w (m/s), and the measured flow through the borehole with a dilution test, Q_{bh}, can be expressed as:

$$Q_{bh} = q_w \cdot L_{bh}^2 \left[r_d \cdot \alpha \cdot \sin\beta + \pi \cdot \cos\beta \left(\frac{a_{D1}}{2} + \frac{a_{D2}}{4} + \frac{a_{D3}}{6} \right) \right] \qquad 2\text{-}2$$

where

$$r_d = \frac{2r_w}{L_{bh}} \qquad 2\text{-}3$$

Assuming a 90° angle between borehole and the flow direction the relationship between

Q_{bh} and q_w may be estimated from

$$Q_{bh} = q_w \cdot L_{bh} \cdot 2r_w \cdot \alpha \qquad 2\text{-}4$$

where L_{bh} is the length of the borehole section (m), r_w is the borehole radius (m) and α is the factor accounting for the distortion of flow caused by the borehole. The factor α was given the value 2 in the calculations, which is the theoretical value for a homogeneous porous media.

2.4.3 Tracer test

The evaluation of the tracer test has involved computer modelling using a simple one-dimensional advection-dispersion model (Van Genuchten & Alves, 1982). From the computer modelling, dispersivity and mean travel times were determined using an automated parameter estimation program, PAREST (Nordqvist, 1994). PAREST uses a non-linear least squares regression where regression statistics (correlation, standard errors and correlation between parameters) also is obtained.

The chosen one-dimensional model assumes a constant fluid velocity and negligible transverse dispersion, cf. Equation 2-5.

$$\partial C/\partial t = D(\partial^2 C/\partial x^2) - v \cdot \partial C/\partial x \qquad 2\text{-}5$$

where: D = Dispersion coefficient
v = fluid velocity (m/s)
C = concentration of solute
x = distance from injection point (m)
t = time (s)

According to Ogata & Banks (1961) and Zuber (1974), the dispersion in a radially converging flow field can be calculated with good approximation by equations valid for one-dimensional flow. Although a linear flow model (constant velocity) is used for a converging flow field, it can be demonstrated that breakthrough curves and parameter estimates are similar for Peclet numbers of about 10 and higher.

Van Genuchten (1982) gives a solution for step input with dispersion over the injection boundary. The solution of Equation 2-5, then is:

$$C/C_o = 2\ \mathrm{erfc}\,[(x-v\cdot t)/Z] + (V/\pi)^2 \exp\,[(x-v\cdot t)^2/(4D\cdot t)] - 2[1+v\cdot x/D+V]\exp\,[v\cdot x/D]\,\mathrm{erfc}[(x+v\cdot t)/Z] \qquad 2\text{-}6$$

where: $Z = 2(D\cdot t)^2$

$V = v^2 t/D$

Variable injection schemes were simulated by superposition of the solution given in Equation 2-6.

The fit of the breakthrough curves using a three-parameter fit included velocity, v, dispersion coefficient, D, and the so called F-factor which corresponds to injected mass divided by fracture volume, M_{inj}/V_f. The result of the evaluation is presented in Chapter 3.7.3.

Based on the mean travel times, t_m, determined from the parameter estimation, the hydraulic fracture conductivity, K_{fr} (m/s), were calculated assuming radial flow and validity of Darcy's law (Gustafsson & Klockars, 1981);

$$K_{fr} = \ln (r/r_w) (r^2 - r_w^2) / 2 \cdot t_m \cdot \Delta h \qquad 2\text{-}7$$

where: r = travel distance (m)
r_w = borehole radius (m)
t_m = mean travel time of tracer (s)
Δh = head difference (m)

The equivalent fracture aperture, b (m), was calculated from:

$$b = Q \cdot t_m / \pi \cdot (r^2 - r_w^2) \qquad 2\text{-}8$$

where Q (m^3/s), is the mean pumping rate.

Flow porosity, θ_k, was calculated using:

$$\theta_k = K/K_{fr} \qquad 2\text{-}9$$

where K is the hydraulic conductivity of the packed-off section of the borehole determined from steady state evaluation of the interference test (Moye, 1967):

$$K = (Q/\Delta h \cdot L) \cdot ((1+\ln L/2r_w)/2\pi) \qquad 2\text{-}10$$

where L (m) is the length of the packed-off section. It should be noted that the term flow porosity might be misleading to use in a fractured heterogeneous rock as it is defined for a porous media. However, it is often used in fractured media as a scaling factor for transport, but then defined over a finite thickness which, in his case, is defined as the length of the packed-off borehole section (L = 1.0 m).

The values calculated using Equations 2-7 through 2-10 are presented together with parameters determined from the numerical modelling of the tracer breakthrough in Table 3-6.

Tracer mass recovery was calculated by integration of the injection and breakthrough curves for mass flux (mg/h) versus time (h).

3 Results and interpretation

3.1 General

The equipment has worked well and no major hydraulic disturbance has occurred during the tests. A few of the sections closest to the I-tunnel have been somewhat disturbed by activities in the G-tunnel during the pumping phase of PT-2. However, this has not affected the interpretation of the tests. A summary of the tests are given in Table 3-1.

Table 3-1. Summary of pre-tests 1-4 (PT-1 – PT-4).

Test #	Sink	Structure	Q* (l/min)	S_p ** (m)	Q/S_p (m^2/s)	Flow period (h)
PT-1	KI0023B:P4	13	0.675	389	$2.9 \cdot 10^{-8}$	24
PT-2	KI0023B:P6	21	2.55	225	$1.9 \cdot 10^{-7}$	48
PT-3	KI0025F02:P5	20	4.70	72	$1.1 \cdot 10^{-6}$	93
PT-4	KI0023B:P6	21	2.40	209***	-	663

* Flow at the end of the pumping period
** Drawdown at the end of the pumping period
*** Influenced by "global" pressure variations

3.2 Pressure response matrix

The pressure response matrix for PT-1 to PT-3 is shown in Figure 3-1. The matrix is based on the responses during the flow phase. The coding in colours and letters is based on the two indexes s_p/Q (drawdown normalised to pumping rate) and t_R/R^2 (response time normalised to the square of the distance) according to Andersson et al. (1998). For PT-1 and PT-3 the drawdown pattern at the end of the flow phase is shown whereas for test PT-2 the data during the flow phase were truncated at t=1140 min due to external disturbances, see below.

Figure 3-1 shows that the pressure responses during PT-1 are restricted to the central area of the block. During PT-2 and PT-3, most of the monitored borehole sections respond. The response patterns during the latter two tests are similar. The difference

between the tests are mainly resulting from the strength of the sink in relation to the distances involved. The hydraulic responses are discussed more in detail for each test below.

Borehole	Interval (m)	Structure #13 PT-1	#21 PT-2	#20 PT-3	Structure
KA2511A:T1	239-293		B	B	#10,11,18
KA2511A:T2	171-238		B	B	#19
KA2511A:T3	139-170		B	B	# ?
KA2511A:T4	111-138		B	B	#20
KA2511A:T5	103-110		B	B	#16
KA2511A:T6	96-102		B	B	#6
KA2511A:T7	65-95		B	B	# ?
KA2511A:T8	6-64		B	B	#4,7
KA2563A:S1	242-246	M	B	B	#19
KA2563A:S2	236-241		B	B	#19
KA2563A:S3	206-208	M	M	G	#13
KA2563A:S4	187-190	M	E	E	#20
KA2563A:S5	146-186	M	G	G	#6,7
KI0025F:R1	169-194		B	B	Z
KI0025F:R2	164-168		B	B	#19
KI0025F:R3	89-163		M	B	?
KI0025F:R4	86-88	M	G	G	# 20
KI0025F:R5	41-85		B	B	#6
KI0025F:R6	3.5-40		B	B	# 5
KI0023B:P1	113.7-200.7		B	B	#10
KI0023B:P2	111.25-112.7		B	B	#19
KI0023B:P3	87.20-110.25	E	E	G	?
KI0023B:P4	84.75-86.20	S	E	M	#13
KI0023B:P5	72.95-83.75	G	G	G	#18
KI0023B:P6	70.95-71.95	B	S	G	#21
KI0023B:P7	43.45-69.95	M	E	E	#6, 20
KI0023B:P8	41.45-42.45		B	M	#7
KI0023B:P9	4.5-40.45			B	#5
KI0025F02:P1	135.15-204		B	B	#?
KI0025F02:P2	100.25-134.15		B	B	#19
KI0025F02:P3	93.40-99.25	B	M	B	#13,21
KI0025F02:P4	78.25-92.4	B	B	B	#?
KI0025F02:P5	73.3-77.25	B	G	S	#20
KI0025F02:P6	64.0-72.3	B	M	M	#22
KI0025F02:P7	56.1-63.0	B	B	M	#?
KI0025F02:P8	51.7-55.1	M	G	G	#6
KI0025F02:P9	38.5-50.7		B	M	#7
KI0025F02:P10	3.4-37.5		B	B	#5
KA3510A:P1	122.02-150				#3,4,5,6,8
KA3510A:P2	114.02-121.02		B	M	#15
KA3510A:P3	4.52-113.02			B	#?
KA3548A01:P1	15-30			B	#?
KA3548A01:P2	10-14			B	#?
KA3573A:P1	18-40		B	B	#15
KA3573A:P2	4.5-17			B	#5
KA3600F:P1	22-50.1			B	#?
KA3600F:P2	4.5-21		B	B	#5, 7?

INDEX 1=sp/Q
EXCELLENT
HIGH
MEDIUM
LOW
NO RESPONSE

INDEX 2=tr/R2
E=EXCELLENT
G=GOOD
M=MEDIUM
B=BAD

S=SOURCE

Figure 3-1. *Pressure response matrix (cf. Andersson et al., 1998) for pre-tests PT-1 to PT-3.*

3.3 Pre-Test #1 (PT-1)

The first test, PT-1, performed by pumping structure #13 in KI0023B:P4, shows pressure responses in 15 borehole sections within the TRUE Block over distances ranging between 15 and 45 m. The pumping flow rate decreased from 0.89 to 0.68 l/min during the 24-hour pumping period. A decrease in the electrical conductivity indicating increasing portion of less saline water was also noted (cf. Figure 3-2).

In the sink borehole, good responses are found in the two sections adjacent to the pumping section (KI0023B:P3 and P5), cf. Figure 3-3. However, both sections have a low transmissivity and may be affected by minor compliance in the equipment caused by the pressure drop in section P4. It should also be noted that section P3 includes the entire water volume of the (collapsed) central tube in the borehole. The latter section has therefore been omitted in the diagnostic pressure response plots. Good responses are also found in sections KI0023B:P6 and P7 in the sink borehole. The latter section contains structures #6 and 20.

In the receiver boreholes, a very good hydraulic response also occur in KA2563A:S3 (#13) as expected, cf. Figure 3-3. The remainder of the responding sections are all, except three, interpreted to contain structures #6, 7, 13, 20, 21 and 22. The remaining three sections include two low-transmissive sections in KI0025F02 (P4 and P7), and one in structure #19 (KA2563A:S1). Notable is also the slow response in KI0025F02:P3 interpreted to include structure #13. In the latter section the flow rate increased significantly during flowing, cf. Table 3-1.

The rather strong pressure response in KI0025F02:P8 (structure #6) may possibly be (in part) explained by the hydraulic short-circuiting in the sink borehole. This may result in that structure #6 also is activated in this borehole during the flow period via section KI0023B:P7, cf. above.

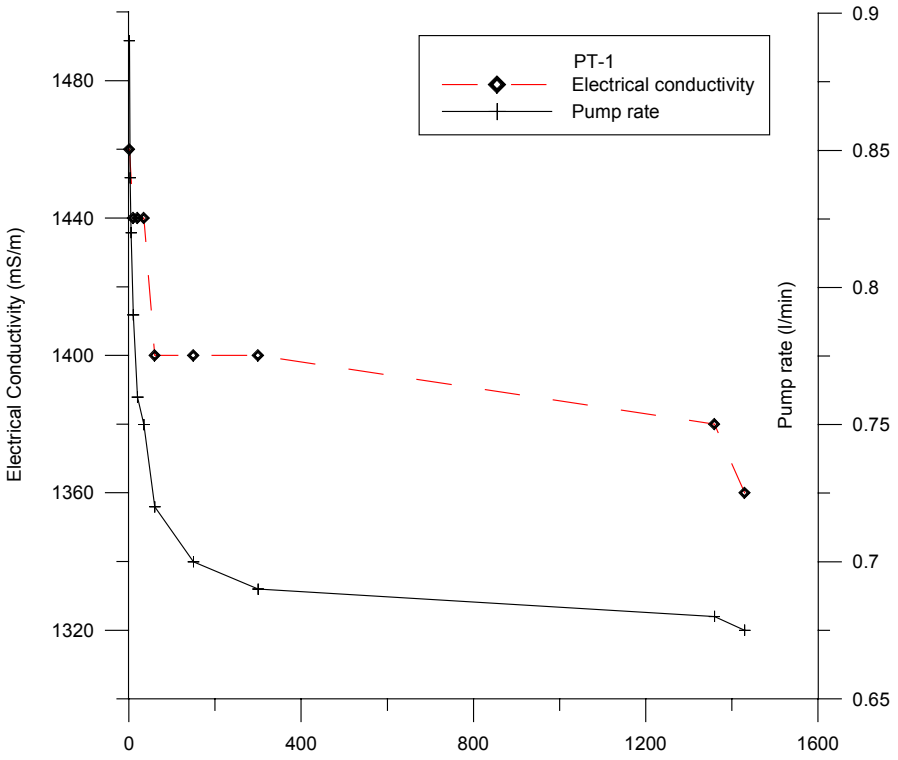

Figure 3-2. *Pump rate and electrical conductivity of pumped water during pre-test PT-1.*

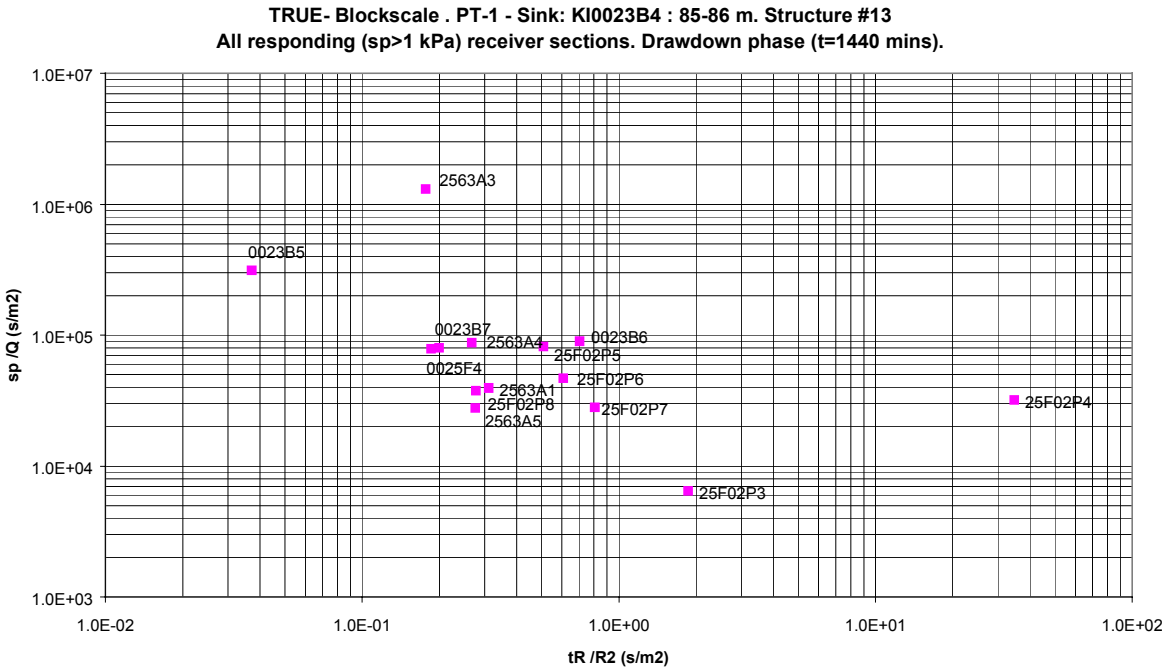

Figure 3-3. *Diagnostic response plot (cf. Andersson et al., 1998) for pre-test PT-1.*

PT-1 also included measurements of flow rates using the tracer dilution method in six selected observation sections. The tests were performed both under natural gradient and during pumping in order to study the influence of the pumping. The results presented in Table 3-2 show a distinct influence in three of the selected sections including structures #13, 20 and 21, whereas two sections have a minor and uncertain increase and one section (KI0025F:R4) has no increase at all. The latter section, which is interpreted in Structure #20, shows a rather strong pressure response, c.f. Figure 3-3. Notable is that section KA2563A:S4 (formerly R5) has a significantly lower (1/4) natural flow than during the measurements in Spring 1998 (Andersson et al., 1998). One possible explanation for this may be the re-instumentation of KA2563A.

The good flow response in KA2563A:S3 and KI0025F02:P3 confirm the structural interpretation of structure #13 and the response in KA2563A:S4 suggests that structures #13 and #20 are better interconnected in the northwestern parts of the block. This is also consistent with the orientation of the two structures.

Table 3-2. Results of tracer dilution tests during PT-1.

Test section	Structure	$Q_{natural}$ (ml/h)	Q_{pump} (ml/h)	ΔQ (ml/h)
KA2563A:S3	13	1	16	+ 15
KA2563A:S4	20	120	280	+ 160
KI0023B:P6	21	36	40	+ 4
KI0025F:R4	20	1	1	± 0
KI0025F02:P3	13,21	38	130	+ 92
KI0025F02:P5	20	49	58	+ 9

The sections with the most significant pressure responses (including the tracer dilution sections) during PT-1 are shown in a drawdown versus time/distance squared (t/R^2)-diagram in Appendix 1. In a homogenous and isotropic medium all response curves would merge to a common curve. The figure shows that medium is heterogeneous. The calculated transmissivity and storativity corresponds to the limiting Theis´-curve shown and thus mainly represent section KA2563A:S3.

Quantitative (time-drawdown) evaluation has been made for the most significant responses of the receiver sections according to the procedures described in Section 2.4.1. The results for PT-1 are shown in Table 3-3. The calculated values of the hydraulic parameters represent parameters of an equivalent fractured porous medium.

It should be observed that the results from receiver sections with small drawdowns, e.g sections located at long distances from the sink section or, alternatively, sections with decreased hydraulic connection to the sink section, are uncertain. In particular, the transmissivity may be over-estimated in such cases due to the assumptions regarding homogeneity and isotropy in the evaluation model. In addition, the results from receiver sections within the sink borehole may be uncertain due to non-radial flow between the sink and receiver sections. Uncertain results due to any of the above reasons are marked with an asterix in Table 3-3. In this table, the transmissivity (T), storativity (S), the hydraulic diffusivity (T/S) and the leakage coefficient (K'/b') are estimated together with the dominating flow geometry during the test.

Table 3-3. Results of quantitative evaluation of hydraulic tests during PT-1. Leaky=pseudospherical, CHB=Apparent Constant head boundary T=transmissivity.

Borehole Section	Structure #	T (m^2/s)	Storativity	T/S (m^2/s)	K'/b' (s^{-1})	Dom. Flow Geometry
KA2563A:S1	19	$3.7\cdot10^{-6}$ *	$1.8\cdot10^{-6}$ *	2.0 *	$5.7\cdot10^{-11}$ *	Leaky→CHB
KA2563A:S3	13	$4.5\cdot10^{-8}$	$8.6\cdot10^{-8}$	0.5	$1.2\cdot10^{-11}$	Leaky
KA2563A:S4	20	$6.9\cdot10^{-7}$	$1.3\cdot10^{-6}$	0.5	$1.1\cdot10^{-10}$	Leaky
KA2563A:S5	6, 7	$1.8\cdot10^{-6}$ *	$1.8\cdot10^{-6}$ *	1.0 *	$1.1\cdot10^{-10}$ *	Leaky→CHB
KI0025F:R4	20	$6.7\cdot10^{-7}$	$8.0\cdot10^{-7}$	0.8	$6.2\cdot10^{-11}$	Leaky
KI0023B:P4 (SINK)	13	$3.2\cdot10^{-7}$	-	-	-	Leaky→CHB
KI0023B:P5	18?	$2.4\cdot10^{-7}$ *	$3.4\cdot10^{-6}$ *	0.07 *	$6.9\cdot10^{-10}$ *	Irregular
KI0023B:P6	21	$6.9\cdot10^{-7}$ *	$3.6\cdot10^{-6}$ *	0.07 *	$2.5\cdot10^{-10}$ *	Leaky
KI0023B:P7	6, 20	$7.5\cdot10^{-7}$ *	$1.1\cdot10^{-6}$ *	0.7 *	$1.4\cdot10^{-10}$ *	Leaky
KI0025F02:P3	13, 21	$6.3\cdot10^{-6}$ *	$1.3\cdot10^{-5}$ *	0.5 *	$1.3\cdot10^{-9}$ *	Leaky→CHB
KI0025F02:P5	20	$7.3\cdot10^{-7}$	$2.0\cdot10^{-6}$	0.4	$2.1\cdot10^{-10}$	Leaky
KI0025F02:P6	22	$1.2\cdot10^{-6}$ *	$2.9\cdot10^{-6}$ *	0.4 *	$2.5\cdot10^{-10}$ *	Leaky
KI0025F02:P8	6	$1.5\cdot10^{-6}$ *	$1.6\cdot10^{-6}$ *	0.9 *	$1.6\cdot10^{-10}$ *	Leaky

* = uncertain value, see discussion above.

3.4 Pre-Test #2 (PT-2)

The second test, PT-2, performed by pumping structure #21 in KI0023B:P6, shows pressure responses in 40 of the 47 monitored borehole sections within the TRUE Block array over distances ranging between 15 and 150 m. The pumping flow rate decreased from 2.85 to 2.55 l/min during the 48-hour pumping period. A decrease in the electrical conductivity indicating increasing portion of less saline water was also noted (cf. Figure 3-4).

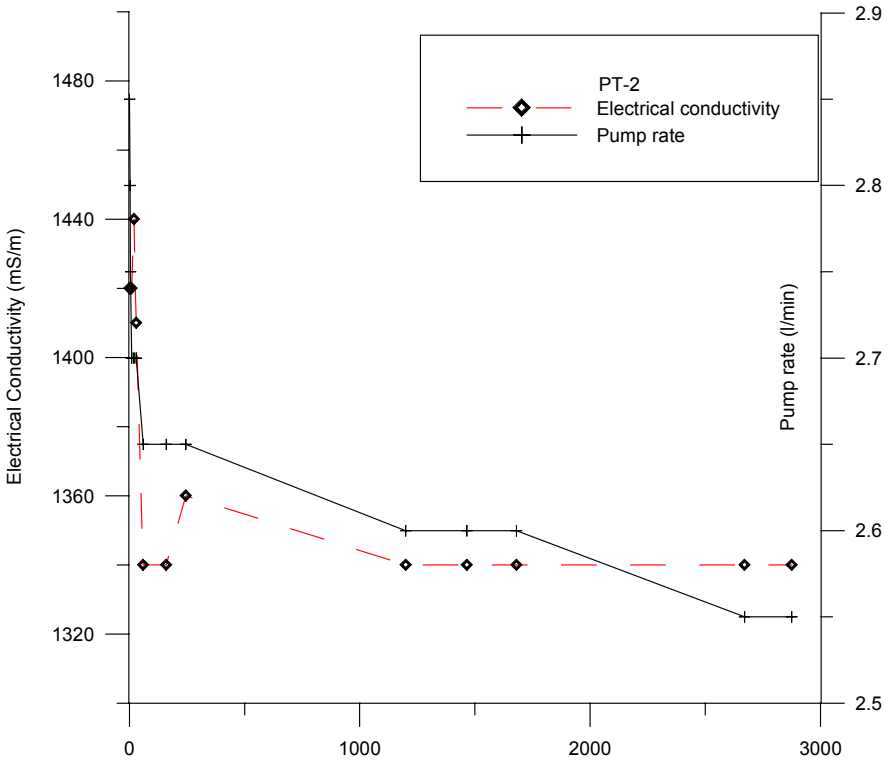

Figure 3-4. *Pump rate and electrical conductivity of pumped water during pre-test PT-2.*

In the diagnostic pressure response plots the data during the flow phase are truncated at t=1140 min due to external interference after this time. In the sink borehole, strong responses occurred in the adjacent sections KI0023B:P3, P4, P5 and P7 to the flowing section P6 (structure #21) which results in that several other structures were (indirectly) activated during this test (structures #6, 13, 18, 20).

In the receiver boreholes, the most prominent responses are found in sections interpreted to include structures #6, 13, 20, 21 and 22, cf. Figure 3-5. The figure shows that the hydraulic connectivity between structures #13, 20, 21 and 22 is very good. The rather strong pressure responses in sections KI0025F02:P8 and KA2563A:S5, containing structures #6 and 7, may possibly (in part) be explained by the hydraulic short-circuiting in the sink borehole, c.f. above.

The remaining responses are lower and slower. Slow pressure responses are observed in sections KA2563:S1 and S2, indicating that structure #19 has a certain hydraulic connection to structure #21, cf. Table 3-3. The non-responding sections are all interpreted to be associated with structure #5 which seems to be hydraulically well isolated from the system formed by #21 and associated structures.

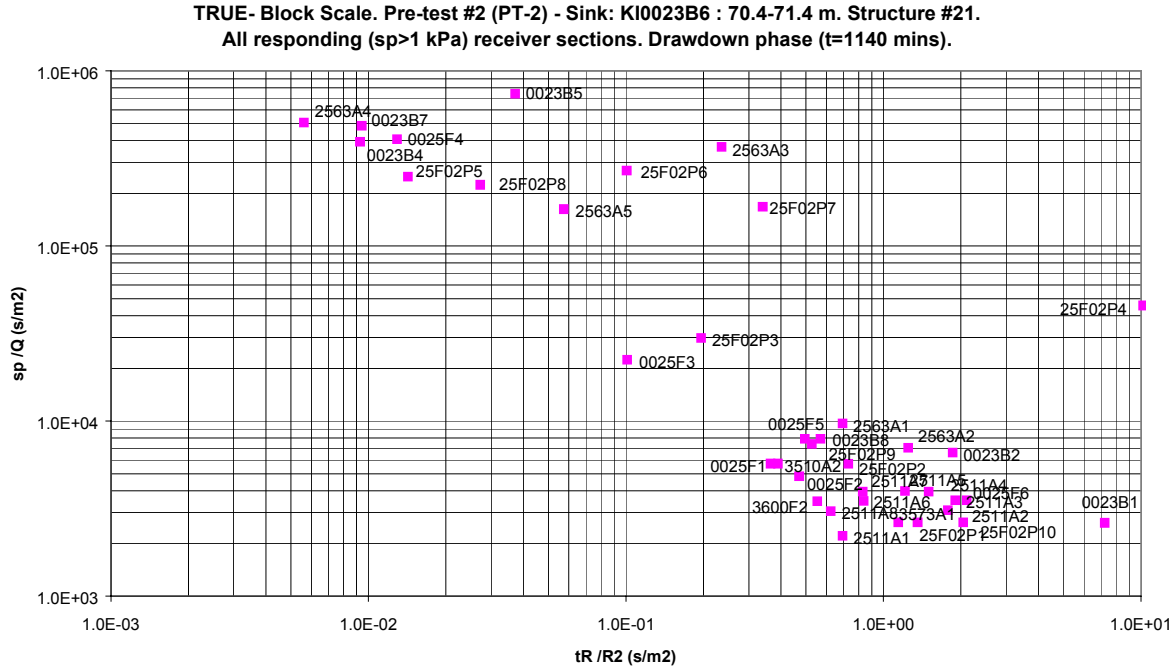

Figure 3-5. *Diagnostic response plot (cf. Andersson et al., 1998) for pre-test PT-2.*

The sections with the most significant pressure responses (including the tracer dilution sections) during PT-2 are shown in a drawdown versus time/distance squared (t/R^2)-diagram in Appendix 1. The calculated transmissivity and storativity corresponds to the limiting Theis´-curve shown and thus mainly represent section KI0025F:R4.

PT-2 included measurements of flow rates using the tracer dilution method in twelve selected observation sections. The tests were performed both under natural gradient and during pumping in order to study the influence of the pumping. The results presented in Table 3-4 show a distinct influence in nine of the selected sections, including structures #6, 13, 19, 20, 21 and 22 whereas three sections have a minor and uncertain increase/decrease. The two remaining sections measured during PT-2 could not be interpreted due to some unknown degradation of the tracer used. In conjunction with PT-4, which uses the same sink as PT-2, some of the uncertainties in the tracer dilution tests were unraveled by repetition of the tests, cf. Table 3-4.

The observed increases are generally very significant but in one case a decrease is observed from 10100 to 2500 ml/h. This section (KI0023B:P7) is adjacent to the sink and is interpreted to include two structures, #6 and #20. The extremely high flow during natural conditions is likely to be caused by the head difference between structures #6 and #20. When pumping starts in the section containing structure #21, the gradient is reversed, or partly reversed. This is further discussed in Chapter 4.

Table 3-4. Results of tracer dilution tests during PT-2.

Test section	Structure	$Q_{natural}$ (ml/h)	Q_{pumped} (ml/h)	ΔQ (ml/h)
KA2563A:S3	13	14	11	– 3
KA2563A:S4	20	130	610	+ 480
KA2563A:S1	19	115	400	+ 285
KI0023B:P4	13	18	16	– 2
KI0023B:P5	?	2	122	+ 120
KI0023B:P7	6,20	10120	2490	– 7630
KI0025F:R4	20	3	1	– 2
KI0025F02:P3	13,21	25	140	+ 115
KI0025F02:P5	20	50	111	+ 61
KI0025F02:P6	22	230	460	+ 230
KI0025F02:P7	?	7	18	+ 11
KI0025F02:P8	6	21	13	– 8

* Value determined during PT-4

The results of the quantitative evaluation of the hydraulic tests in PT-2 are shown in Table 3-5. The same comments apply as for PT-1, see Section 3.3. As for the qualitative analysis, the drawdown responses during PT-2 were truncated due to external disturbances, see above.

Table 3-5. Results of the quantitative evaluation of hydraulic test responses during PT-2. T=transmissivity, Leaky=pseudospherical, CHB=Apparent Constant head boundary, Tidal=Response clearly affected by tidal effects.

Borehole Section	Structure #	T (m^2/s)	Storativity	T/S (m^2/s)	K'/b' (s^{-1})	Dom. Flow Geometry
KA2563A:S1	19	$2.4 \cdot 10^{-5}$ *	$1.7 \cdot 10^{-5}$ *	1.4 *	-	Radial→Tidal
KA2563A:S3	13	$6.0 \cdot 10^{-7}$	$2.3 \cdot 10^{-6}$	0.3	$1.6 \cdot 10^{-10}$	Leaky
KA2563A:S4	20	$7.4 \cdot 10^{-7}$	$2.0 \cdot 10^{-7}$	3.6	$2.7 \cdot 10^{-11}$	Leaky
KA2563A:S5	6, 7	$1.5 \cdot 10^{-6}$ *	$8.9 \cdot 10^{-7}$ *	1.7 *	$1.8 \cdot 10^{-10}$ *	Leaky
KI0025F:R4	20	$8.1 \cdot 10^{-7}$	$1.1 \cdot 10^{-7}$	7.5	$8.7 \cdot 10^{-12}$	Leaky
KI0023B:P4	13	$6.0 \cdot 10^{-7}$ *	$3.8 \cdot 10^{-6}$ *	0.2 *	$2.1 \cdot 10^{-10}$ *	Leaky
KI0023B:P5	18	$4.7 \cdot 10^{-7}$ *	$1.3 \cdot 10^{-6}$ *	0.4 *	$1.2 \cdot 10^{-10}$ *	Leaky
KI0023B:P6 (SINK)	21	$1.2 \cdot 10^{-6}$	-	-	-	Leaky→CHB
KI0023B:P7	6, 20	$7.9 \cdot 10^{-7}$ *	$2.4 \cdot 10^{-7}$ *	3.3 *	$2.4 \cdot 10^{-11}$ *	Leaky
KI0025F02:P3	13, 21	$1.0 \cdot 10^{-5}$ *	$3.8 \cdot 10^{-6}$ *	2.7 *	$2.1 \cdot 10^{-10}$ *	Leaky→CHB
KI0025F02:P5	20	$7.7 \cdot 10^{-7}$	$1.9 \cdot 10^{-7}$	4.0	$2.9 \cdot 10^{-11}$	Leaky
KI0025F02:P6	22	$1.1 \cdot 10^{-6}$	$7.4 \cdot 10^{-7}$	1.5	$1.5 \cdot 10^{-10}$	Leaky
KI0025F02:P7	?	$1.2 \cdot 10^{-6}$	$3.6 \cdot 10^{-6}$	0.3	$4.4 \cdot 10^{-10}$	Leaky
KI0025F02:P8	6	$1.4 \cdot 10^{-6}$	$3.8 \cdot 10^{-7}$	3.7	$7.6 \cdot 10^{-11}$	Leaky

* = uncertain value, see discussion above

3.5 Pre-Test #3 (PT-3)

The third test, PT-3, performed by pumping structure #20 in KI0025F02:P5, shows pressure responses in 46 of the 47 monitored borehole sections within the TRUE Block array over distances ranging between 15 and 150 m.. The pumping flow rate was kept rather constant throughout the 48-hour pumping period, at about 4.8 l/min. The electrical conductivity was also almost constant, 1440 mS/m, cf. Figure 3-6.

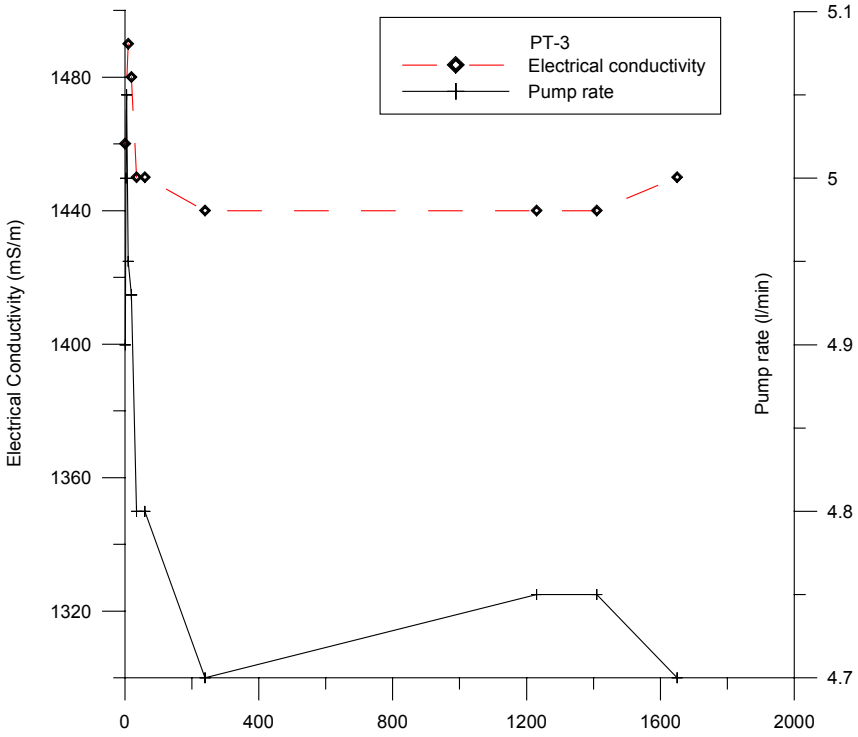

Figure 3-6. *Pump rate and electrical conductivity of pumped water during pre-test PT-3.*

The response pattern for this test is very similar to test PT-2, cf. Figure 3-1. This implies that structures #20 and 21 have a very good hydraulic connection.

The most prominent responses are found in sections interpreted to include structures #6, 7, 13, 20, 21 and 22, cf. Figure 3-7. The remaining responses are lower and slower. The same conclusions can be drawn from this test as for the previous test.

The sections with the most significant pressure responses (including the tracer dilution sections) during PT-3 are shown in a drawdown versus time/distance squared (t/R^2)-diagram in Appendix 1. The calculated transmissivity and storativity corresponds to the limiting Theis´-curve shown and thus mainly represent section KA2563A:S4.

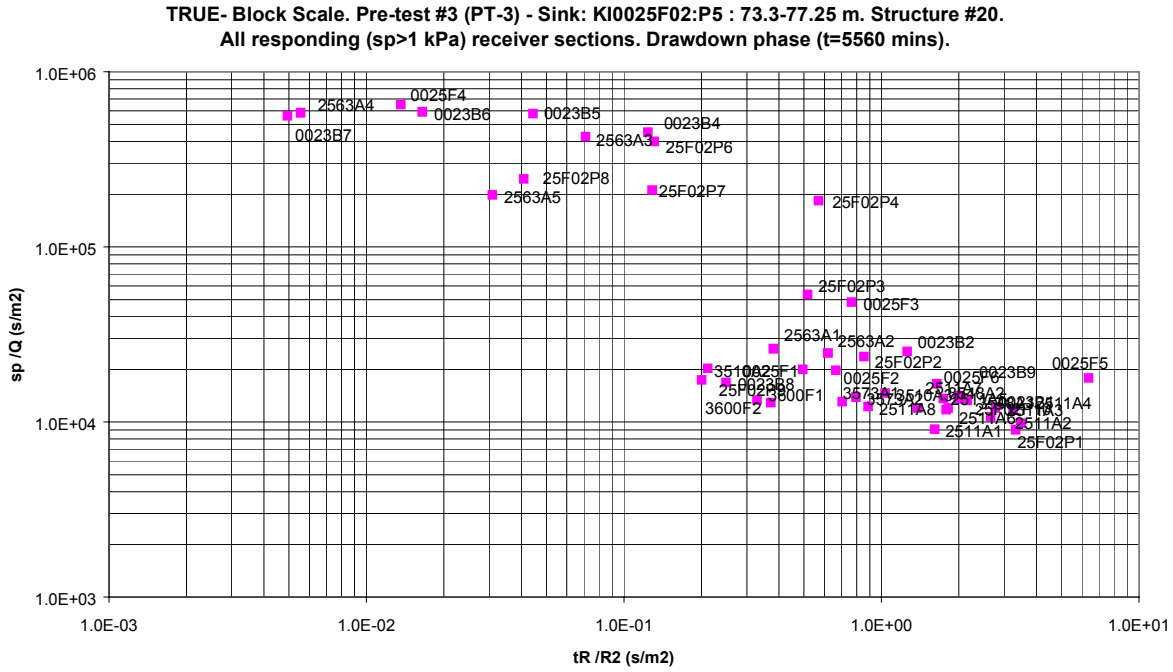

Figure 3-7. *Diagnostic response plot (cf. Andersson et al., 1998) for pre-test PT-3.*

PT-3 included measurements of flow rates using the tracer dilution method in twelve selected observation sections. The test were performed both under natural gradient and during pumping in order to study the influence of the pumping. The results presented in Table 3-6 show a distinct influence in five of the selected sections containing structures #6, 13, 20, 21 and 22 whereas one section (KI0025F02:P8) has a minor and uncertain increase and one (KI0023B:P2) has no increase. Section KI0025F02:P3 could only be measured during the pumping phase but is most likely also influenced by the pumping as the natural flow during PT-1 and PT-2 was significantly lower than 250 ml/min, cf. Tables 3.1 and 3.3. The four remaining sections could not be interpreted due to some unknown degradation of the tracer used.

Table 3-6. Results of tracer dilution tests during PT-3. Values within brackets are uncertain. Questionmarks represent bad data.

Test section	Structure	$Q_{natural}$ (ml/h)	Q_{pumped} (ml/h)	ΔQ (ml/h)
KA2563A:S3	13	?	15	?
KA2563A:S4	20	80	950	+ 870
KI0023B:P2	19	14	14	± 0
KI0023B:P4	13	?	?	?
KI0023B:P5	?	(390)	(90)	– 300
KI0023B:P6	21	3	12	+ 9
KI0023B:P7	6,20	?	?	?
KI0025F:R4	20	3	5	+ 2
KI0025F02:P3	13,21	?	250	+ 200?
KI0025F02:P6	22	100	1500	+ 1400
KI0025F02:P7	?	?	?	?
KI0025F02:P8	6	33	39	+ 6

The results of the quantitative evaluation of the hydraulic tests in PT-3 are shown in Table 3-7. The same comments apply as for PT-1, see Section 3.3. Notable is also the clear effects of no-flow hydraulic boundaries occurring in most of the responding sections (including the sink) at about 2000 minutes (33 hours) during the drawdown phase, cf. Appendix A. The boundary effect is not as pronounced during the recovery phase but can be seen in some sections. In section KI0025F02:P3, no-flow boundary effects appear earlier, at about 250 minutes (4 hours), both during drawdown and recovery. Such boundary effects have not been seen in previous tests of KI0025F02:P5 (Adams et al., in prep.) but considering the long duration of the drawdown phase (4 days) they might represent large-scale effects, i.e. limitations in the extension of the fracture system tested.

Table 3-7. Results of the quantitative evaluation of hydraulic test responses during PT-3. T=Transmissivity, Leaky=pseudospherical, NFB=Apparent No-flow boundary.

Borehole Section	Structure #	T (m^2/s)	Storativity	T/S (m^2/s)	K'/b' (s^{-1})	Dom. Flow Geometry
KA2563A:S3	13	$6.0 \cdot 10^{-7}$	$9.5 \cdot 10^{-7}$	0.6	$4.8 \cdot 10^{-11}$	Leaky→NFB
KA2563A:S4	20	$7.0 \cdot 10^{-7}$	$7.4 \cdot 10^{-8}$	9.5	$8.3 \cdot 10^{-12}$	Leaky→NFB
KA2563A:S5	6, 7	$1.4 \cdot 10^{-6}$	$5.5 \cdot 10^{-7}$	2.6	$5.5 \cdot 10^{-11}$	Leaky→NFB
KI0025F:R4	20	$6.5 \cdot 10^{-7}$	$2.1 \cdot 10^{-7}$	3.1	$6.6 \cdot 10^{-12}$	Leaky→NFB
KI0023B:P4	13	$6.3 \cdot 10^{-7}$	$2.2 \cdot 10^{-6}$	0.3	$1.2 \cdot 10^{-10}$	Leaky→NFB
KI0023B:P5	18	$6.5 \cdot 10^{-7}$	$5.4 \cdot 10^{-7}$	1.2	$3.7 \cdot 10^{-11}$	Leaky→NFB
KI0023B:P6	21	$7.3 \cdot 10^{-7}$	$2.1 \cdot 10^{-7}$	3.4	$2.7 \cdot 10^{-11}$	Leaky→NFB
KI0023B:P7	6, 20	$7.8 \cdot 10^{-7}$	$1.2 \cdot 10^{-7}$	6.7	$9.8 \cdot 10^{-12}$	Leaky→NFB
KI0025F02:P3	13, 21	$1.0 \cdot 10^{-5}$ *	$1.3 \cdot 10^{-5}$ *	0.8 *	$1.5 \cdot 10^{-9}$ *	Leaky→NFB
KI0025F02:P5 (SINK)	20	$6.9 \cdot 10^{-7}$	-	-	-	Leaky→NFB
KI0025F02:P6	22	$1.0 \cdot 10^{-6}$ *	$2.2 \cdot 10^{-6}$ *	0.4 *	$2.0 \cdot 10^{-10}$ *	Leaky→NFB
KI0025F02:P7	?	$1.3 \cdot 10^{-6}$ *	$5.1 \cdot 10^{-6}$ *	0.2 *	$5.6 \cdot 10^{-10}$ *	Leaky→NFB
KI0025F02:P8	6	$1.5 \cdot 10^{-6}$ *	$5.8 \cdot 10^{-7}$ *	2.6 *	$6.1 \cdot 10^{-11}$ *	Leaky→NFB

* = uncertain value, see discussion above.

3.6 Pre-PT-4

Prior to the actual tracer injections during PT-4, two tracer injections were performed in KI0023B:P7 with the purpose to check that the pumping in KI0023B:P6 is strong enough to reverse the hydraulic gradient in section P7 caused by the short-circuit between structures #6 and #20 in the latter section. Figure 3-8 shows a schematic plane view of borehole KI0023B and the intercepts with different structures.

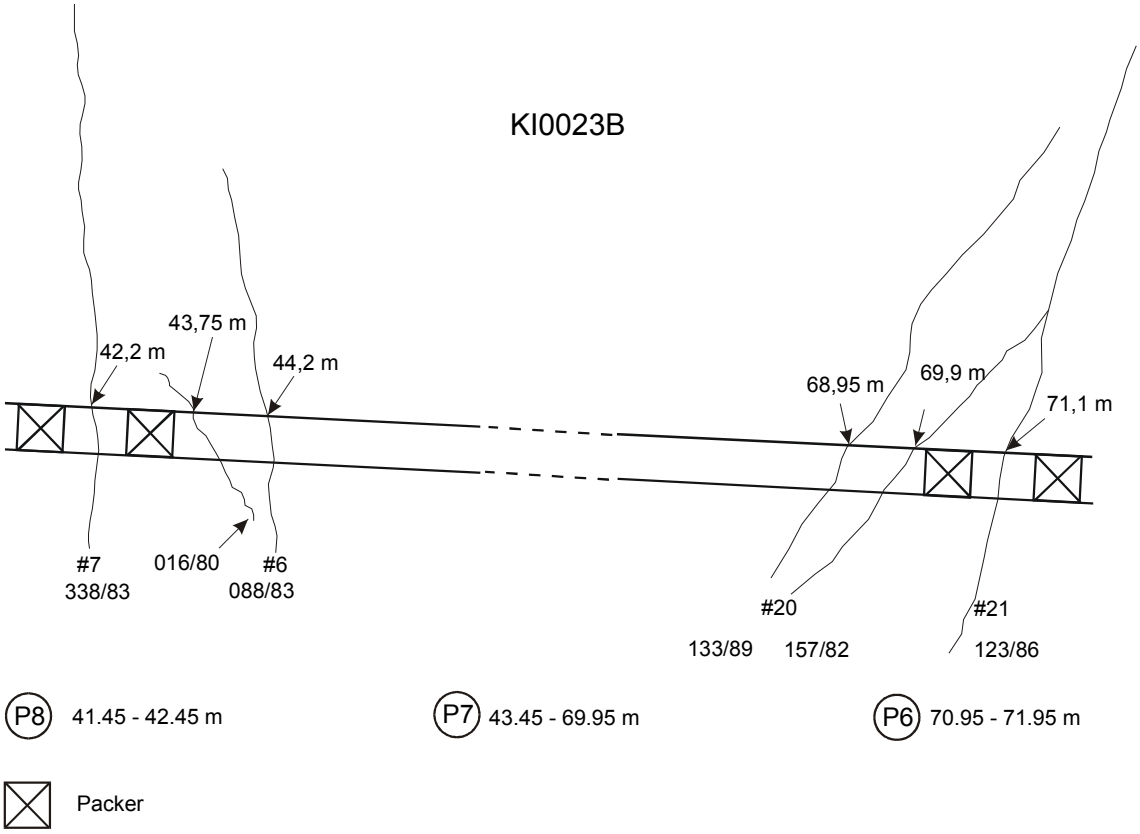

Figure 3-8. *Schematic plane view of borehole KI0023B with fracture intersections in the packed-off sections P6, P7 and P8.*

The first injection was performed by injecting a slug of Uranine in the lower part of section P7, close to structure #20, and the second by injecting a slug of Rhodamine WT close to structure #6 in the upper part of section P7. The injections were made through the circulation loop. Pumping was done in KI0023B:P6 with the same pumping rate as in PT-2.

The breakthrough of Uranine (Figure 3-9) shows a very fast travel time with a first arrival of about 10 minutes. The injection was originally intended to cover the entire length of the section but as breakthrough was clearly visible, the injection was stopped after 25 minutes. The additional small peak after 2 hours results from an unintentional run of the circulation pump creating a short extra pulse. The peak after 4 hours corresponds to the injection of Rhodamine in the upper part of the borehole which was performed by switching the inlet and outlet tubes of the circulation loop. Thus, Uranine remaining in the tube was also injected simultaneously with the Rhodamine pulse. The tracer mass recovery of Uranine was estimated to 100%.

The results confirms that structures #20 and #21 intersect very close to the borehole which also is indicated by the orientation of the structures obtained from the BIPS measurement (Figure 3-8).

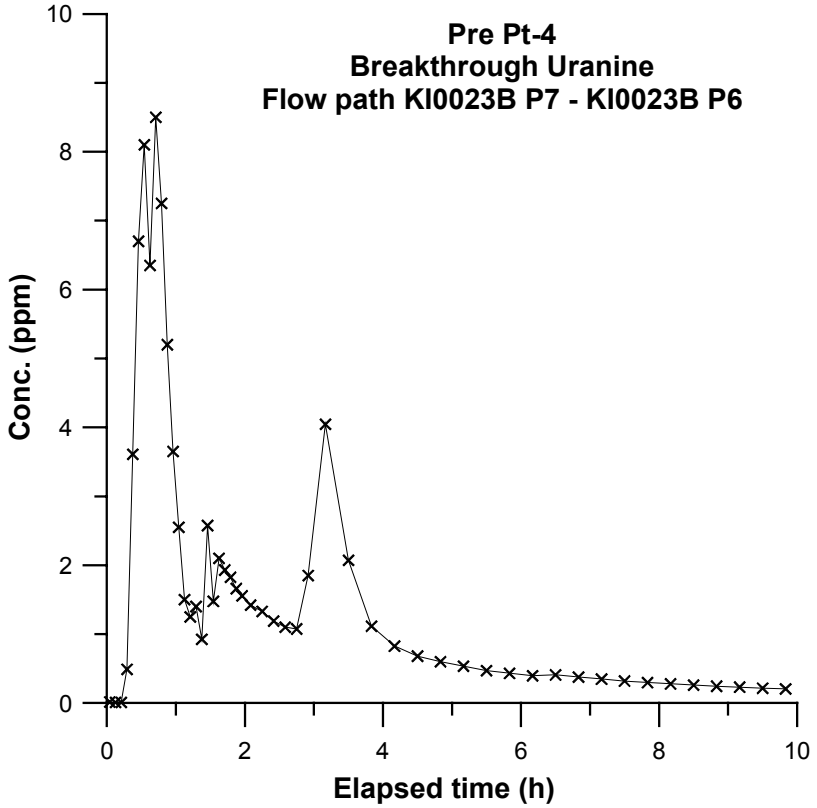

Figure 3-9. *Breakthrough of Uranine in KI0023B:P6 from injection in the lower part of section P7, close to structure #20, cf. Figure 3-8.*

The breakthrough of Rhodamine WT from the upper part of section P7 (Figure 3-10) is delayed with about 1-2 hours compared to the Uranine breakthrough which corresponds to the travel time along the 27.5 m long borehole section. The breakthrough confirms that water from structure #6 flows along the borehole section. However, the tracer mass recovery of Rhodamine WT was estimated to only about 50% indicating that parts of the tracer mass is lost. Losses could occur either to other fractures intersecting the borehole that are controlled by an even stronger sink than section P6, or by entrappment in poorely mixed parts of the section (no circulation was done).

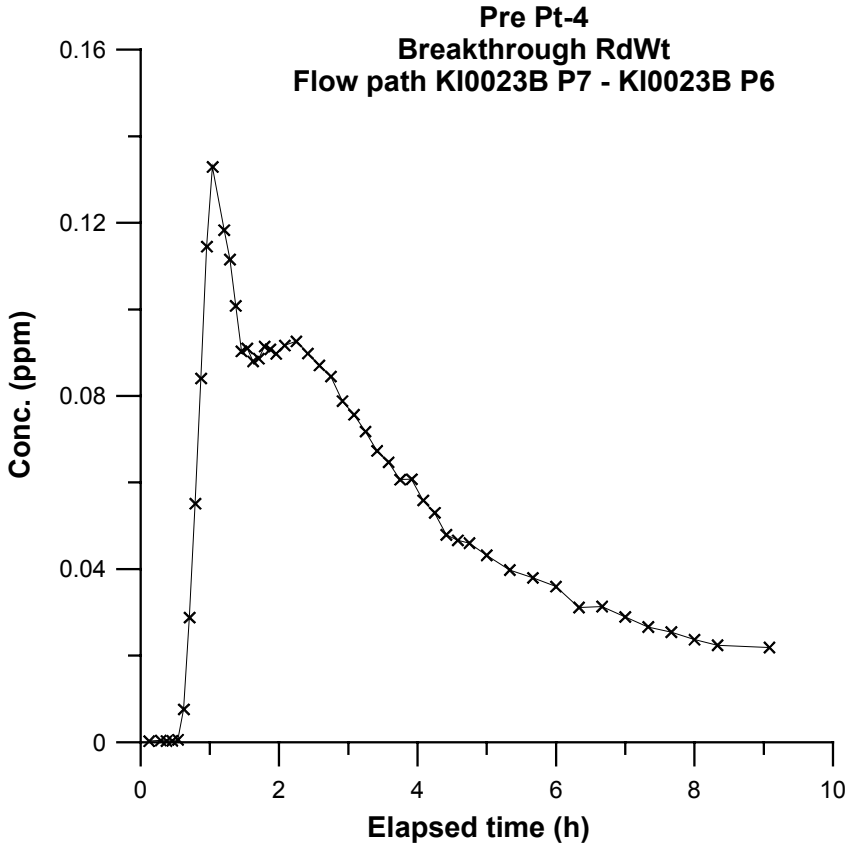

Figure 3-10. *Breakthrough of Rhodamine WT in KI0023B:P6 from injection in the upper part of section P7, close to structure #6, cf. Figure 3-8.*

3.7 Pre-Test #4 (PT-4)

The fourth pre-test, PT-4, was focused on tracer transport. Based on the many good flow responses observed during PT-2 (Table 3-4) the same set-up was decided for use in PT-4. Pumping was done in KI0023B:P6 with the same pumping rate as in PT-2 and four primary injection sections were chosen (Table 3-8). An optional injection section was also selected, but it was decided to limit the number of tracers injected to avoid contamination and also to optimise the analysis resourses available.

3.7.1 Tracer injections

The injections were performed as decaying pulses. In two of the injections (sections KI0025F02:P3 and KI0025F02:P6), the tracer solution was exchanged with non-traced water in order to shorten the tail of the breakthrough curve. However, due to the relatively large volume of the circulating system a rather poor efficiency was obtained. The injection concentrations and injection rates given in Table 3-8 are the actually measured ones.

Table 3-8. Tracer injection data for PT-4 (measured values).

Inj #	Section	Structure	Tracer	Max Inj conc(mg/l)	Inj rate (ml/h)*	Vol. of sect. (ml)
1	KA2563A:S4	20	Rhodamine	120	680	6883
2	KA2563A:S1	19	Uranine	420	220	8814
3	KI0025F02:P3	13, 21	Amino G Acid	2200	113	8238
4	KI0025F02:P6	22	Rhodamine	250	350	9717

*Calculated from the tracer dilution during injection

The injection functions presented as the logarithm of concentration (Ln C) versus time are shown in Figure 3-11.

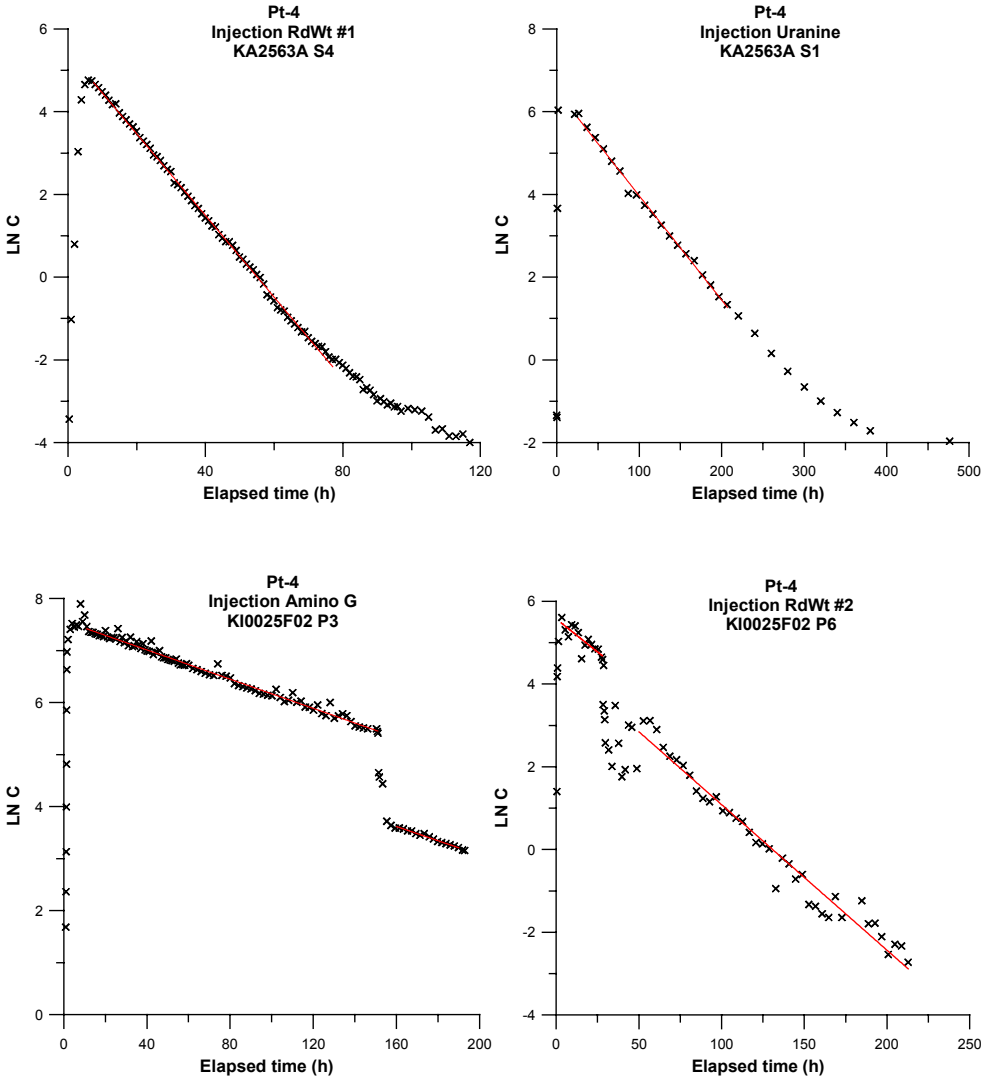

Figure 3-11. *Tracer injection functions (Ln C versus time) including straight-line fits for the four injections during PT-4. Note that the axis scales differ.*

3.7.2 Tracer breakthrough

The breakthrough of tracer was monitored both in the sink section KI0023B:P6 and in the adjacent section P7, where the short-circuit between structure #6 and #20 occurs. Tracer breakthrough was detected from all four injections in section P6 and the resulting breakthrough curves are presented in Figure 3-12.

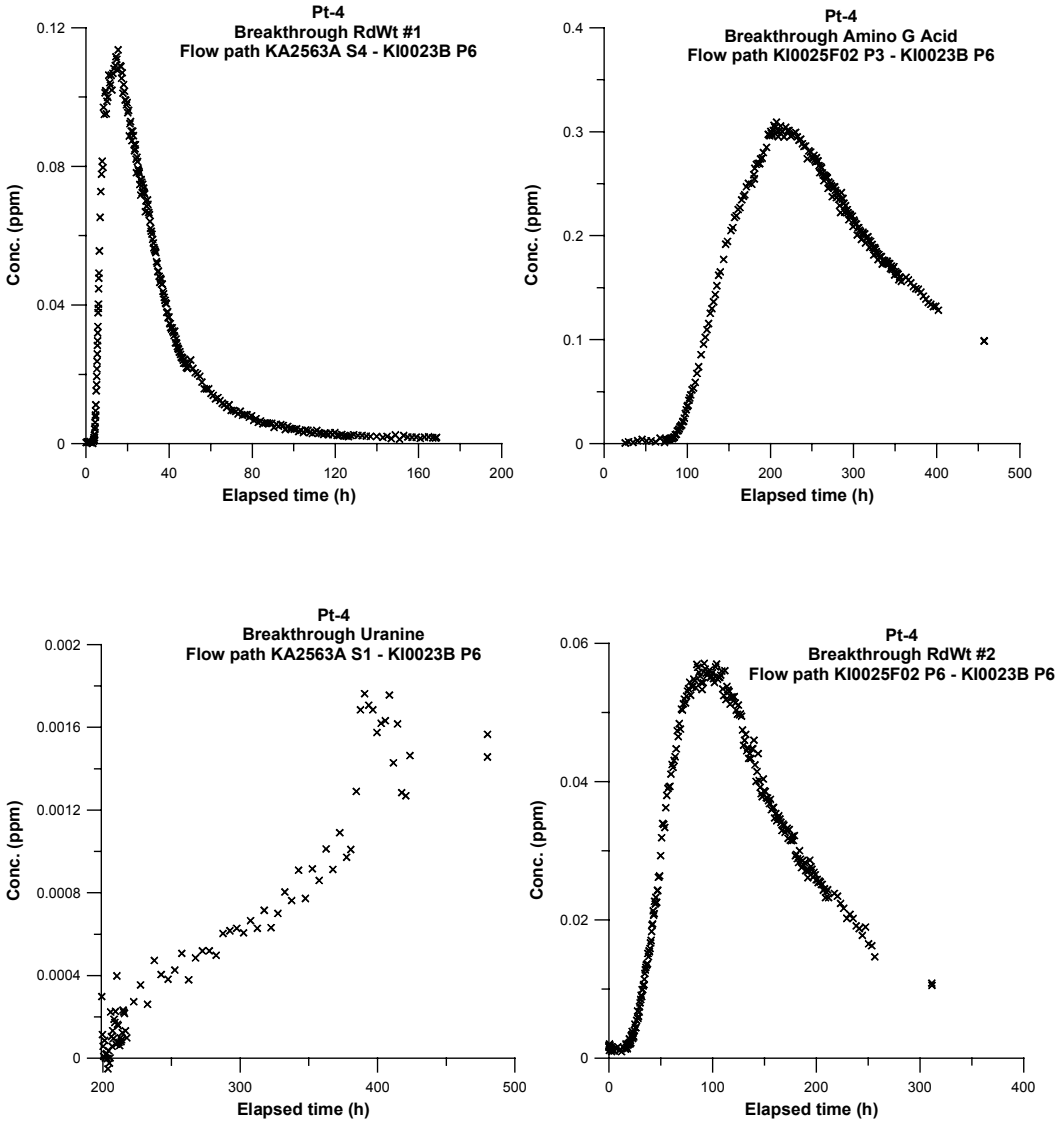

Figure 3-12. *Tracer breakthrough in KI0023B:P6 during PT-4. Note that the axis scales differ between the plots.*

The pumping was stopped on June 15th after a pumping period of 28 days. The equipment was removed to Uppsala for cleaning and maintenance. No major equipment failure occurred during the test period.

Calculations of the tracer mass recovery (Table 3-9) show high mass recovery for two of the flow paths (>75%). A rather large portion of the tail of the breakthrough then still remains to be recovered, and it is therefore likely that the mass recovery would have raised up close to 100%. The mass recovery of Rhodamine WT from KA2563A:S4 only reaches about 50%, i.e. only slightly higher than during ESV-1c (Andersson et al., 1998) although the discharge from KI0023B:P6 is 2.5 times higher (2.5 l/min compared to 1.0 l/min during ESV-1c). Finally, the mass recovery of Uranine from structure #19 in KA2563A:S1 is still less than 1% after 480 hours. It is likely that the flow path from the injection point to the sink is very long and complicated as several structures need to be crossed.

No tracer breakthrough was found in KI0023B:P7 during the pumping period.

Table 3-9. Tracer mass recoveries from KI0023B:P6 during PT-4.

Inj #	Section	Structure	Tracer	Mass Recovery (%)	Sampling time (h)
1	KA2563A:S4	20	Rhodamine WT	51	169
2	KA2563A:S1	19	Uranine	<1	480
3	KI0025F02:P3	13, 21	Amino G Acid	75*	457
4	KI0025F02:P6	22	Rhodamine WT	80*	311

* mass recovery likely to be close to 100% if sampling had been prolonged

3.7.3 Numerical modelling and analytical interpretation

The breakthrough curves from PT-4 were evaluated using the one-dimensional advection-dispersion model described in Section 2.4.3.

The transport parameters derived from the numerical modelling and the analytical expressions described in Section 2.4.3 are presented in Table 3-10. The parameters for the flow path KA2563A:S4 → KI0023B:P6 from PT-4 are also compared to those obtained from the tracer test performed in the same flow path during ESV-1c, in April 1998 (Andersson et al., 1998), cf. Table 3-11. Borehole KA2563A was re-instrumented in March 1999 and the present borehole section KA2563A:S4 corresponds to the previous section KA2563A:R5, both containing structure #20.

The best-fit runs for each tracer/flow path are presented in Figure 3-13. The modelling resulted in relatively good fits with quite low standard errors, 0.5-4 %. In general the peak of the breakthrough curves is quite well fitted while the tail part is worse.

Numerical modelling for the flow path KA2563A:S1 → KI0023B:P6 has not been made since the tracer mass recovery of Uranine was very low and no complete breakthrough curve was obtained.

Table 3-10. Summary of hydraulic and transport parameters for the flow paths KA2563A:S4 – KI0023B:P6, KI0025F02:P3 - KI0023B:P6 and KI0025F02:P6 - KI0023B:P6 in PT-4. Values within brackets are standard errors in percent.

Parameter	KA2563A:S4 -KI0023B:P6 Value	KI0025F02:P3 -KI0023B:P6 Value	KI0025F02:P6 -KI0023B:P6 Value	Source
Travel distance, L (m)	16	36	18	Geometry
Mean head difference, Δh (m)	190	214.5	203.5	HMS
Mean velocity, v (m/s)	$3.9 \cdot 10^{-4}$ (1)	$7.1 \cdot 10^{-5}$ (0.5)	$4.5 \cdot 10^{-5}$ (0.5)	PAREST
Mean travel time, t_m (h)	11.5 (1)	140.3 (0.5)	98.3 (0.5)	PAREST
First arrival, t_a (h)	4	85	19	Breakthrough curve
Dispersivity, D/v (m)	5.3 (3.6)	2.9 (4.1)	5.0 (1)	PAREST
Peclet number, Pe	3.0	12.6	3.6	PAREST
Fracture conductivity, K_{fr} (m/s)	$9.8 \cdot 10^{-5}$	$4.1 \cdot 10^{-5}$	$1.4 \cdot 10^{-5}$	Eq. 2-7
Equivalent fracture aperture, b (m)	$2.2 \cdot 10^{-3}$	$5.2 \cdot 10^{-3}$	$1.4 \cdot 10^{-2}$	Eq. 2-8
Flow porosity (1 m thickness)	$1.1 \cdot 10^{-3}$	$2.7 \cdot 10^{-3}$	$8.0 \cdot 10^{-3}$	Eq. 2-9
Mass recovery, R (%)	51	75	80	Breakthrough curve

Table 3-11. Comparison between hydraulic and transport parameters for flow path KA2563A:S4 – KI0023B:P6 from PT-4 and KA2563A:R5 - KI0023B:P6 from ESV-1c. Values within brackets are standard errors in percent.

Parameter	PT-4 Value	ESV-1c Value	Source
Travel distance, L (m)	16	16	Geometry
Mean head difference, Δh (m)	190	54	HMS
Mean velocity, v (m/s)	$3.9 \cdot 10^{-4}$	$1.9 \cdot 10^{-4}$	PAREST
Mean travel time, t_m (h)	11.5	23.5	PAREST
First arrival, t_a (h)	3.8	10.8	Breakthrough curve
Dispersivity, D/v (m)	5.3	1.6	PAREST
Peclet number, Pe	3	10	PAREST
Fracture conductivity, K_{fr} (m/s)	$1.0 \cdot 10^{-4}$	$1.7 \cdot 10^{-4}$	Eq. 2-7
Equivalent fracture aperture, b (m)	$2.2 \cdot 10^{-3}$	$1.9 \cdot 10^{-3}$	Eq. 2-8
Flow porosity (1 m thickness)	$1.1 \cdot 10^{-3}$	$0.9 \cdot 10^{-3}$	Eq. 2-9
Mass recovery , R (%)	51	44	Breakthrough curve
Pumping rate (l/min)	2.5	1.0	Measured

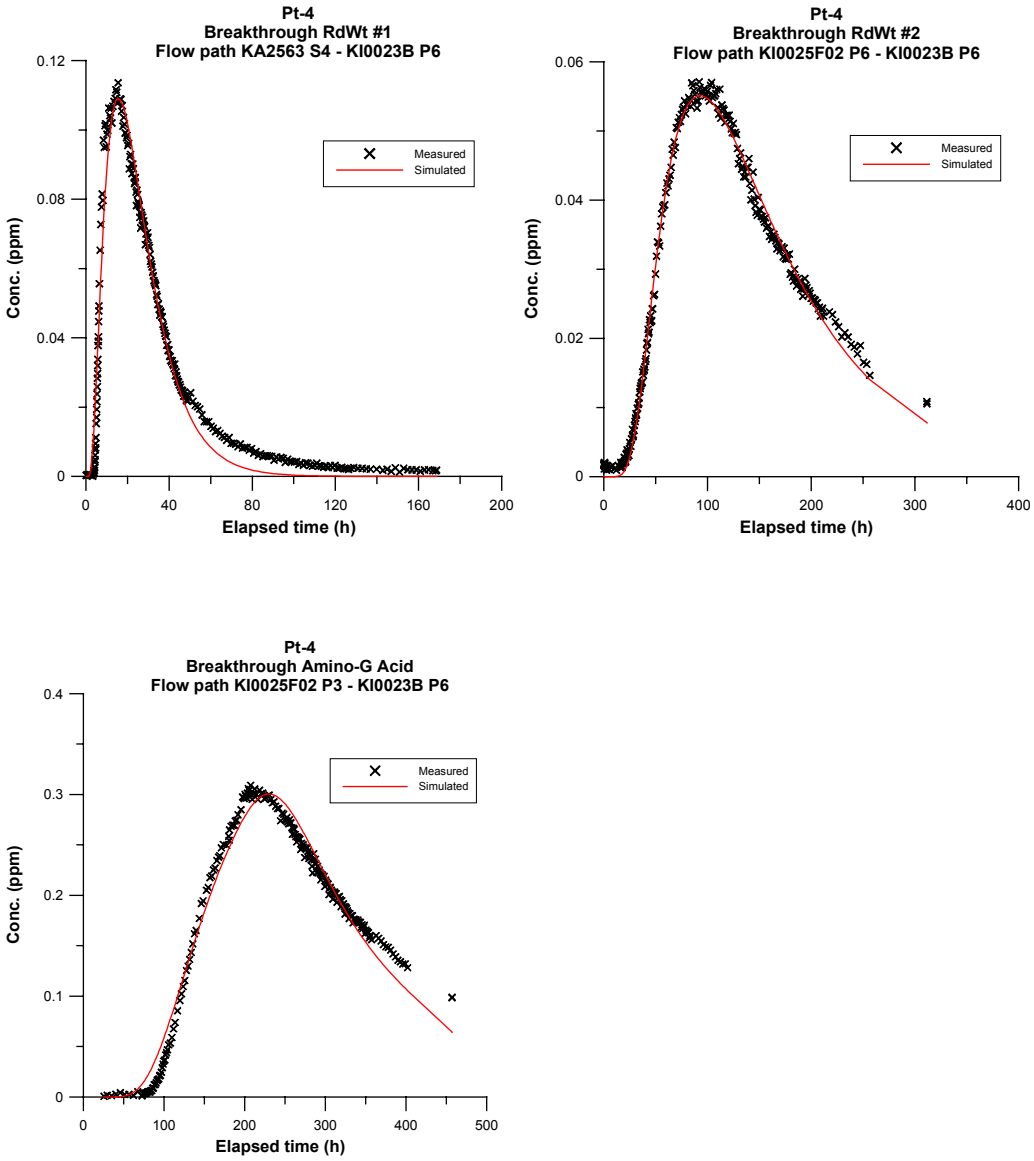

Figure 3-13. *Comparison between measured and simulated tracer breakthrough in KI0023B:P6 during PT-4, cf. Table 3-10 for evaluated parameters. Note that the axis scales differ between the plots.*

4 Conclusions and recommendations for future tests

4.1 Connectivity and structural model

The three pre-tests PT-1, PT-2 and PT-3 generally confirm the March´99 structural model. In most cases, the flow and pressure responses give the same indication of connectivity, i.e. a good (high and fast) pressure response and a good flow response (increase). However, there are exceptions in each test where a low and slow pressure response is obtained together with a good flow response, or the opposite. These results imply that pressure responses alone cannot be used for assessment of transport connectivity. These particular cases are discussed below.

PT-1, performed by pumping structure #13 (KI0023B:P4), shows good flow and pressure responses both within the pumped structure as well as in structures #20 and #21. The only exception being section KI0025F02:P3 where a very good flow response and a slow pressure response is obtained. One possible explanation for this may be that the section is located close to a constant head boundary, which also is indicated by the qualitative interpretation of the pressure response. It should also be noted that this section is intersected both by structures #13 and #21, thus creating a short-circuit between the two structures in the particular section.

PT-2 (and PT-4), performed by pumping structure #21 (KI0023B:P6), gives good flow and pressure responses in structures #6, 13, 20, 21 and #22. The only unexpected response is the significant flow response in structure #19 (KA2563A:S1) which has a relatively low and slow pressure response. Thus, connectivity between structures #21 and #19 clearly exists. This was also confirmed by the tracer breakthrough obtained during PT-4. Two sections containing structures not identified in the March´99 model, KI0023B:P5 and KI0025F02:P7, also show good flow and pressure responses. Possible candidate structures need to be assessed from BIPS measurements and flow logs.

The third test, PT-3, performed by pumping structure #20 (KI0025F02:P5), has an almost identical pressure response pattern as seen in PT-2. Both pressure and flow responses are stronger due to the stronger sink but the pattern is identical. This indicates that KI0025F02 may be used as sink in future tracer tests.

4.2 Hydraulic parameters

The quantitative analysis of the most prominent pressure responses generally shows predominant radial flow with a slight leakage by the end of the test. Analysis of responses in the bounding structures #6, 7 and 19 shows effects of constant head boundaries. In PT-3, indications of no flow boundaries are evident in all responses. This

may indicate a limited extent of structure #20 possibly ending to the east of borehole KI0025F and that the unknown structure in KI0025F02:P7 also is ended to the west of KI0025F02.

The transmissivity and diffussivity values determined are generally rather uniform for structure #20 ($T=7\text{-}12\cdot10^{-7}$ m^2/s, $T/S=3\text{-}10$ m^2/s). They are also consistent with earlier interpretations (Andersson et al., 1998 and Adams et al., in prep). Structure #21, only interpreted in KI0023B:P6 and KI0025F02:P3, gives a similar point value in KI0023B:P6 whereas the low and slow response in KI0025F02:P3 gives an indication of a higher transmissivity ($T=6\text{-}10\cdot10^{-6}$ m^2/s) in that part. The responses in the bounding structures #6, 7 and 19 generally yield about one order of magnitude higher transmissivity values than estimated for structures #13, 20, 21 and 22.

4.3 Transport parameters

The tracer dilution tests in 14 different sections showed that the "natural" flow varies quite a lot within the Block Scale rock volume. An extremely high flow rate (10 l/h) was measured in KI0023B:P7 where a short-circuit between structures #6 and #20 exists. The flow rates in the other measured sections typically were in the range 1-200 ml/h.

Based on the measured flow rates, the Darcy velocity was estimated as described in Chapter 2.4.2. The Darcy velocities determined together with estimates of the hydraulic conductivity, presented in Table 4-1, where used to calculate the hydraulic gradient, *I*. The estimated gradients are typically in the order of 0.3-3 m/m. The exceptions are a few sections connected to structures #20 and #21 having a lower gradient and an extremely high gradient in the short-circuit section KI0023B:P7.

The tracer test performed by pumping in structure #21 (KI0023B:P6) resulted in tracer breakthrough from all four injection points, KA2563A:R1 (structure #19), KA2563A:S4 (structure #20), KI0025F02:P3 (structures #13 and 21) and KI0025F02:P6 (structure #22). The tests cover Euclidean distances ranging between 16 to 36 m which probably are longer in reality.

Very high mass recovery was obtained for the injections in KI0025F03:P3 and P6 whereas the short flow path from KA2563A:S4 only gave 50% mass recovery which should be compared to 44% obtained in a previous test (Andersson et al., 1998). The mass loss is attributed to the boundary conditions (intersections with other structures having lower hydraulic head).

The numerical modelling using a simple one-dimensional advection-dispersion model was not able to fit the breakthrough curves very well. In addition, dispersivity values where unrealistically high for a single path model for two of the modelled flow paths.

Usage of a multiple-path model would improve the fits considerably although this could not be done within the framework of this evaluation. The transport parameters calculated based on the mean travel times; fracture conductivity, equivalent fracture aperture and flow porosity, show somewhat different values, where the flow path from KI0025F02:P6 shows a slow transport, indicating high flow porosity (and large equivalent aperture) whereas the fast flow path from KA2563A:S4 has about one order of magnitude lower flow porosity (and equivalent aperture).

Table 4-1. Summary of measured flow rates, calculated Darcy velocities and hydraulic gradients from PT-1 to PT-4.

Section	Structure	Measured flow (ml/h)	Darcy velocity (m/s)	Hydraulic cond.(m/s)*	Hydr. Gradient (m/m)	Test
KA2563A:S1	19	115	$7.1 \cdot 10^{-8}$	$8.1 \cdot 10^{-8}$	0.9	PT-2
KA2563A:S3	13	14	$1.7 \cdot 10^{-8}$	$1.6 \cdot 10^{-8}$	1.1	PT-2
KA2563A:S4	20	130	$1.1 \cdot 10^{-7}$	$1.3 \cdot 10^{-7}$	0.9	PT-2
KI0023B:P2	19	14	$1.8 \cdot 10^{-8}$	$6.8 \cdot 10^{-8}$	0.3	PT-3
KI0023B:P4	13	18	$2.3 \cdot 10^{-8}$	$1.9 \cdot 10^{-8}$	1.2	PT-2
KI0023B:P5	?	2	$3.4 \cdot 10^{-11}$	$1.6 \cdot 10^{-9}$	0.02	PT-2
KI0023B:P6	21	3	$5.5 \cdot 10^{-9}$	$1.3 \cdot 10^{-7}$	0.04	PT-3
KI0023B:P7	6,20	10000	$6.9 \cdot 10^{-7}$	$3.8 \cdot 10^{-9}$	180	PT-2
KI0025F:R4	20	3	$2.7 \cdot 10^{-9}$	$1.8 \cdot 10^{-8}$	0.15	PT-2 PT-3
KI0025F02:P3	13,21	25	$7.8 \cdot 10^{-9}$	$6.7 \cdot 10^{-9}$	1.2	PT-2
KI0025F02:P5	20	50	$2.3 \cdot 10^{-8}$	$2.8 \cdot 10^{-7}$	0.08	PT-1 PT-2
KI0025F02:P6	22	200	$3.0 \cdot 10^{-8}$	$2.4 \cdot 10^{-8}$	1.2	PT-2
KI0025F02:P7	?	7	$1.8 \cdot 10^{-9}$	$1.2 \cdot 10^{-9}$	1.5	PT-2
KI0025F02:P8	6	21	$1.1 \cdot 10^{-8}$	$3.2 \cdot 10^{-9}$	3.5	PT-2

*= determined from detailed flow logging

4.4 Optimisation of the borehole array

4.4.1 Re-mediation of KI0023B

The results of the tracer dilution tests in KI0023B:P7 clearly indicates that there is a major short-circuit between structures #6 and #20 in the borehole section. The measured "natural" flow rate is in the order of 10 l/h in the direction from #20 to #6, i.e. towards the tunnel. This is also consistent with the hydraulic head measurements which indicate a 5-m head difference between the two structures. However, the tracer dilution tests and the pre-PT-4 tests indicate that the gradient in P7 can be reversed by pumping in section P6.

This means that tracer tests may be performed with KI0023B:P6 used as a sink, which also is manifested by the results of PT-4. However, if another sink is used it may be more difficult to control the head field and avoid tracers being lost. A brief study of the head distribution during PT-3 (KI0025F02:P5 as sink) shows that the head in section P6 is somewhat lower than in section P7 (about 20 kPa) during pumping. Thus, the gradient should still be directed towards P6. A different choice of sink than in PT-4 would most probably require further pre-tests to assess the possibility of performing tracer tests.

Another uncertainty related to KI0023B is the unknown structure in section P5 which is located in between structures #13 and #21. The results of PT-1 to PT-3 and the previous test (Andersson et al., 1998) shows that section P5 is well connected to the neighbouring structures. This is a potentially interesting tracer injection point but the exact location is not known from the 5-m packer logging. This also implies that the packers need to be re-arranged.

In summary, it is possible to perform tracer tests without re-mediation of KI0023B but the consequences of choosing another sink than KI0023B:P6 need to be further explored. The flowing structure in section P5 cannot be used as potential injection point without removing and re-arranging the packer system.

4.4.2 Borehole KI0025F

The latest update of the structural model (March-99) by Hermanson (in prep) includes a structure (#22) that is currently located beneath the packer between section R4 and R3 at 88.8 m borehole length. During flow logging in 5-m intervals (Gentzschein, 1997) a flow rate of 1.08 l/min was measured in the interval 87-92 m. Later, during the pressure build-up tests, a localisation of the flowing structure was made (Gentzschein & Morosini, 1998) where the main flow was located to the section 87.0-87.75 m. However, the detailed localisation was stopped at 88.75 m, i.e. very close to the #22 intercept. The flow was also measured by Andersson & Wass (1998) who found a flow rate of 0.72 l/min at 42 bars pressure drop. The flow rates may be somewhat difficult to compare as boundary conditions are different but, there is a possibility that the noted flow difference is associated with the interpreted structure #22.

One way of exploring this situation would be to simply push the entire instrumentation in KI0025F in two steps of one metre and measure the resulting flow. That means that the packers are moved from the original position at 86-88 m, involving only structure #20, to 87-89 m involving both structures, and finally to 88-90 m involving only structure #22. If #22 is located a short-term interference test should be done.

4.4.3 Borehole KI0025F02

The last update of the March-99 model also includes a dual intercept of structure #21 and #13 in borehole section KI0025F02:P3. The structures are relatively well-separated (4 m) and are easily identified in the detailed POSIVA flow log. Based on the results of the tracer dilution tests and the tracer test during PT-4 it is clear that this section is very interesting for future tracer tests. A separation of the two structures would possibly further increase the understanding of the structures and maybe also increase the number of possible tracer injection points.

Another observation is that the "natural" flow rate measured in this section (25-40 ml/h) is relatively high in comparison with other structures with similar transmissivity. This may indicate that the short-circuit between the structures induces a gradient with an increased flow rate as a result. However, it should be noted that the head difference between the structures probably is much less than in KI0023B:P7.

In summary, the instrumentation of KI0025F02 seems to be well optimised with the exception of the section mentioned above. It should also be noted that the structure at 93.9 m (#13) has about one order of magnitude lower transmissivity than structure #21 at 97.9 m. Thus, it is likely that the main part of the transport occurs in structure #21. The orientation of the two structures also indicates that they intersect not far from the borehole.

Based on the discussion above, a separation of the two structures in section P3 may not be warranted in relation to what could be gained in terms of new injection points.

4.5 Need for a new borehole

The tracer tests performed during PT-4 and the dilution tests performed during PT-1 to PT-3 clearly shows that there are several potential tracer injection points in the current array. From this point of view there is a limited need for a new borehole. There are, however, a few arguments for drilling a new borehole. These are:

- The inter-distances between injection and sinks are rather long, from 16 metres and upwards in the current array. This may limit the number of possible pathways for injection of sorbing tracers

- The borehole intercepts with the target structures line up more or less at the same depth in the array. This means that anisotropy in the system cannot be studied

5 References

Adams, J., Andersson P., Meier P., in prep.: TRUE Block Scale Project. Preliminary results of selective pressure build-up tests in borehole KI0025F02. Äspö Hard Rock Laboratory International Progress Report IPR-01-56.

Andersson, P., 1996: TRUE 1st stage tracer test programme. Experimental data and preliminary evaluation of the TRUE-1 radially converging tracer test (RC-1). Äspö Hard Rock Laboratory Progress Report HRL-96-24.

Andersson, P., Ludvigson, J-E., Wass, E., 1998: TRUE Block Scale Project. Preliminary Characterisation Stage. Combined Interference Tests and Tracer Tests. Appendix volume. Evaluation plots and data sheets for interference test interpretation. Äspö Hard Rock Laboratory International Progress Report IPR-01-44.

Andersson P, Wass E, 1998: TRUE 1st stage tracer test programme. Preliminary Design Tests for tests with radioactive sorbing tracers (PDT-1, PDT-2, PDT-3). Experimental description and preliminary evaluation. Äspö Hard Rock Laboratory Progress Report HRL-98-13.

Gentzschein, B., 1997: TRUE Block Scale Project. Detailed flow logging of core borehole KA2563A.SKB Internal Report.

Gentzschein, B., Morosini, M., 1998: TRUE Block Scale Project. Selective pressure build-up tests in borehole KI0025F. Äspö Hard Rock Laboratory International Progress Report IPR-01-45.

Gustafsson, E., Klockars, C-E., 1981: Studies of groundwater transport in fractured crystalline rock under controlled conditions using non-radioactive tracers. Swedish Nuclear Fuel and Waste Management Company. SKBF/KBS Technical Report TR 81-07

Hermanson, J., in prep.: TRUE Block Scale Project. Structural model March 1999, Based on borehole data from KI0025F02, KA3600F and KA3573A. SKB Internal Report.

Moye, D.G., 1967: Diamond drilling for foundation exploration. Civil Eng. Trans., Inst. Eng. Australia (Apr. 1967), 95-100.

Nordqvist, R., 1994: Documentation of some analytical flow and transport models implemented for use with PAREST - Users manual. GEOSIGMA GRAP 94 006, Uppsala.

Ogata, A., Banks, R., 1961: A solution to the differential equation of longitudinal dispersion in porous media. U.S. Geol. Surv. Prof. Paper 411-A, Washington.

APPENDIX 1: Drawdown versus t/R^2 plots for PT-1, PT-2 and PT-3

GEOSIGMA AB P.O. Box 894 S-751 08 Uppsala Sweden	Pumping test analysis Theis analysis method Confined aquifer	Page 1 Project: TRUE BLOCK SCALE Evaluated by: JEL | Date: 14.06.1999
Pumping Test No. PT-1. Sink:KI0023B:P4	Test conducted on: 1999-04-15	
Drawdown vs. t/R2 (Primary responses)		

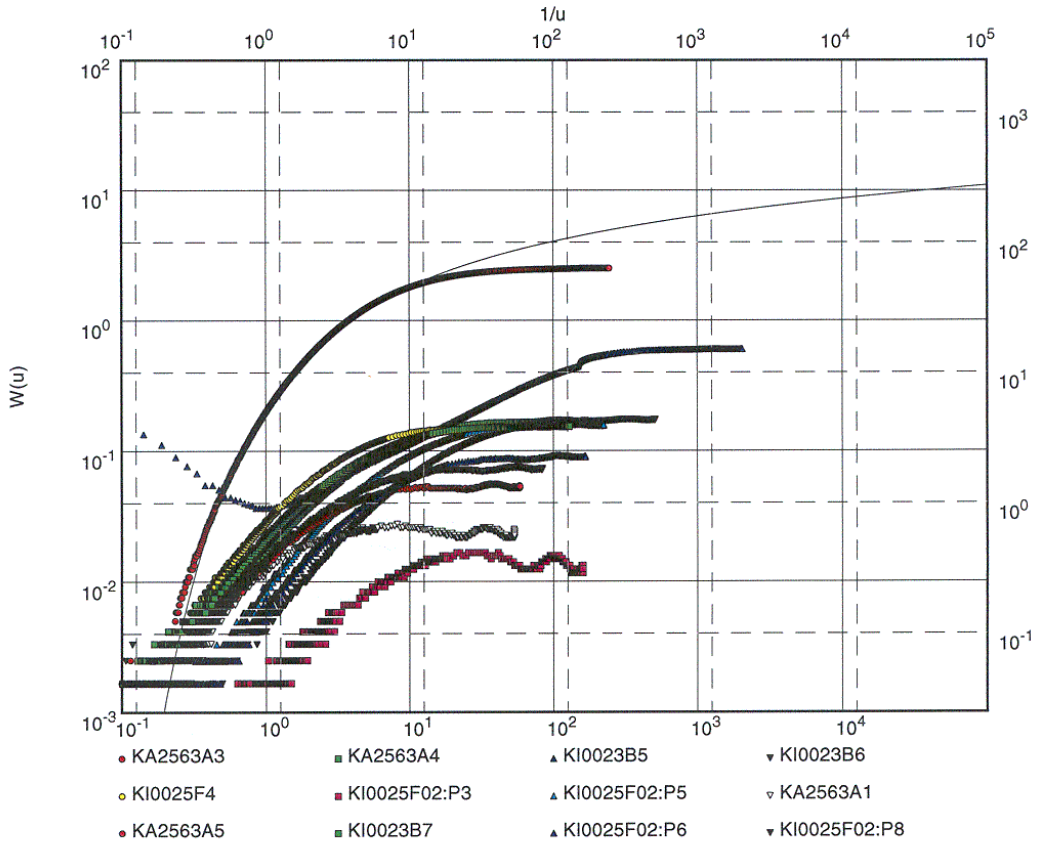

T=4.68E-8 m2/s S=1.48E-7 tp=1440 mins

Data curves: X-axis: time/distance squared (s/m2)
Y-axis: Drawdown (m)

Theis' type curve shown as limiting curve

GEOSIGMA AB P.O. Box 894 S-751 08 Uppsala Sweden	Pumping test analysis Theis analysis method Confined aquifer	Page 1 Project: TRUE BLOCK SCALE Evaluated by: JEL | Date: 25.05.1999
Pumping Test No. PT-2. Sink:KI0023B:P6		Test conducted on: 1999-04-21
Drawdown-t/r2. (Primary responses)		

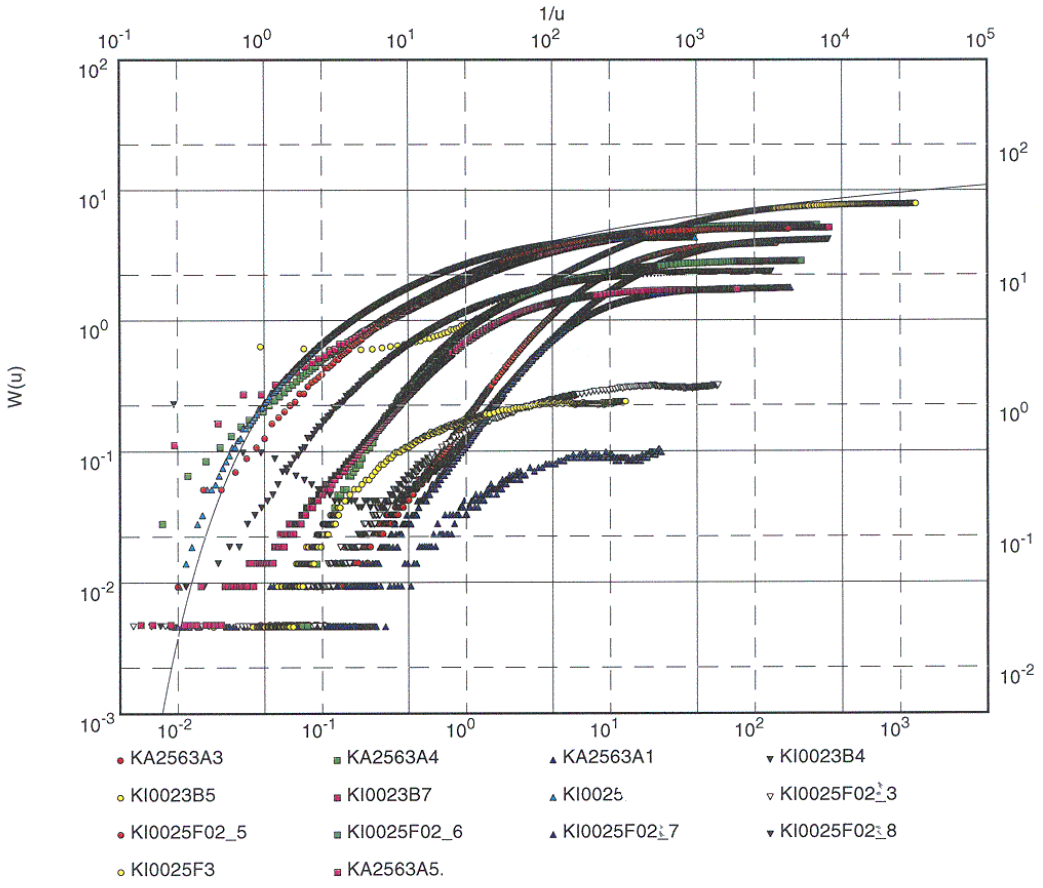

T=8.46E-7 m2/s S=1.34E-7

Data curves: X-axis: time/distance squared (s/m2)
Y-axis: Drawdown (m)

Drawdown data set truncated at t=1140 mins
(68 400 s) due to interference of external activities in the tunnel.

Theis type curve shown as limiting curve.

GEOSIGMA AB P.O. Box 894 S-751 08 Uppsala Sweden	Pumping test analysis Theis analysis method Confined aquifer	Page 1 Project: TRUE BLOCK SCALE Evaluated by: JEL | Date: 15.06.1999
Pumping Test No. PT-3. Sink:KI0025F02:P5	Test conducted on: 1999-04-29	
Drawdown vs. t/R2 (Primary responses)		

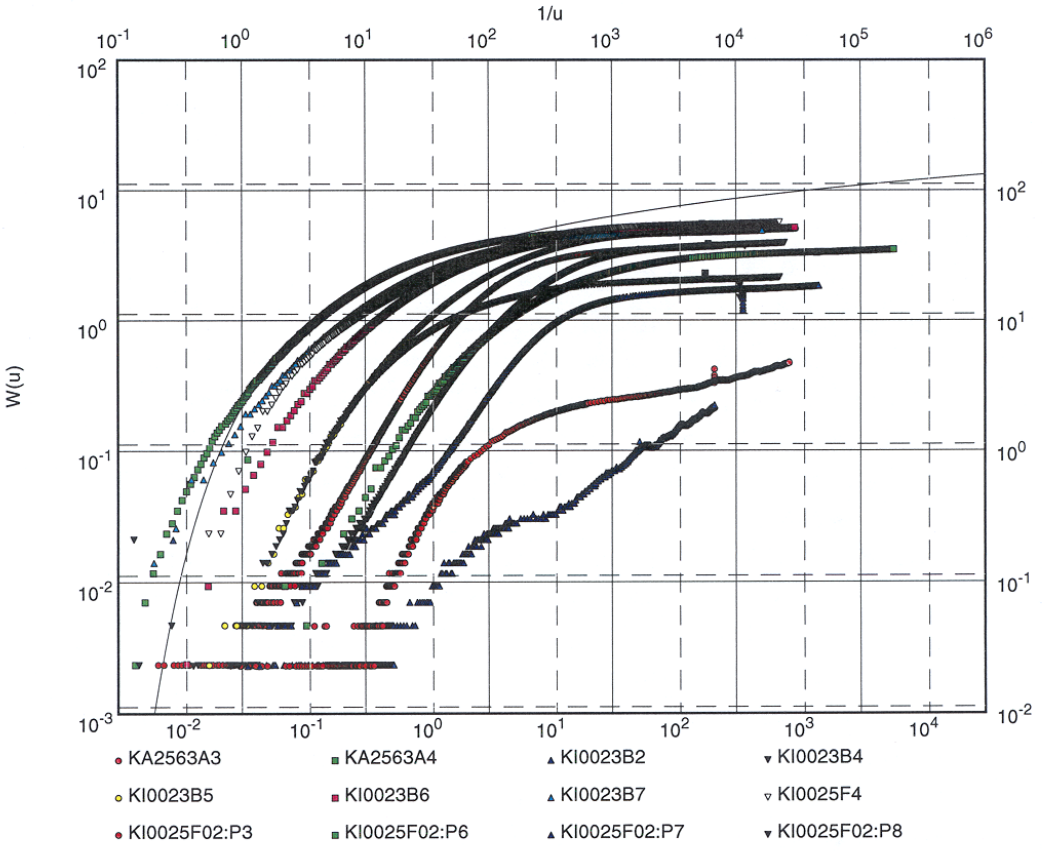

T=6.96E-7 m2/s S=7.85E-8 tp=5560 mins

Data curves: X-axis: time/distance squared (s/m2)
Y-axis: Drawdown (m)

Theis' type curve shown as limiting curve